GA-A13557
UC-77

# EVALUATION OF BISO AND TRISO COATED $ThO_2$ FUEL PARTICLES IRRADIATED IN HFIR CAPSULES HT-12 THROUGH HT-15 AND HT-17 THROUGH HT-19

by
C. B. SCOTT



Prepared under
Contract EY-76-C-03-0167
Project Agreement No. 17
for the San Francisco Operations Office
Department of Energy

GENERAL ATOMIC PROJECT 3224
DATE PUBLISHED: OCTOBER 1977

GENERAL ATOMIC COMPANY

---

ABSTRACT

The HT-12 through HT-15 and HT-17 through HT-19 capsules were uninstrumented experiments conducted in the target position of the High Flux Isotope Reactor at Oak Ridge National Laboratory. The experiments were utilized as evaluation tests of fertile particle coating designs and PyC properties and they provide a basis for normalization of fuel particle design and performance models. A total of thirteen different BISO $ThO_2$ particle designs were irradiated to fast neutron fluences ranging from 1.8 to 14.6 x $10^{25}$ $n/m^2$ $(E > 29\ fJ)_{HTGR}$ and heavy metal burnups ranging from 1.0 to 15.8% FIMA at temperatures of 1025° to 1580°C.

The results indicated that BISO $ThO_2$ particles can be fabricated to survive the most severe large HTGR design irradiation conditions and that anisotropy of the OPyC coating, which is a strong function of coating rate, is one of the most important variables affecting the irradiation performance of BISO coated fertile particles.

CONTENTS

FIGURES

## TABLES

# 1. INTRODUCTION

The HT-12 through HT-15 and HT-17 through HT-19 capsule series were part of a continued cooperative effort between General Atomic Company (GA) and Oak Ridge National Laboratory (ORNL) and were funded by the DOE-sponsored HTGR Fuels and Core Development Program. The experiments were conducted in the target position (HT) of the High Flux Isotope Reactor (HFIR) at ORNL. The capsules were uninstrumented and contained relatively small sample sizes (40 to 75 particles); however, they had the advantage of low cost and achieved peak LHTGR fast neutron exposures and burnups in approximately 3 months. Consequently, these experiments were evaluation tests of LHTGR fertile particle coating designs.

Each capsule contained four magazines that were designed to achieve graphite crucible temperatures of 900° or 1250°C, which correspond to particle temperatures of approximately 1100° and 1500°C. A total of 32 unbonded fertile particle samples containing 41 to 75 fuel particles were tested in each capsule. Sixteen particle samples in each capsule were fabricated by GA and the remainder were ORNL specimens.

The experimental test matrix for the GA fuel particle specimens was established to evaluate the relationship between fuel particle irradiation performance and various coating attributes which included outer pyrocarbon coating (OPyC) density, anisotropy, and coating rate. Some of the coating designs tested were nonconservative in order to establish failure criteria required for coated particle performance model studies. The fuel specimens were predominantly BISO coated $ThO_2$ particles. However, one batch of TRISO coated $ThO_2$ particles, which is the LHTGR backup fertile particle design, was tested in capsules HT-17, HT-18, and HT-19 for comparative purposes.

The capsules were irradiated for two to seven HFIR cycles to fast neutron fluences ranging from 1.8 to 14.6 x $10^{25}$ $n/m^2$ $(E > 29\ fJ)_{HTGR}$ and heavy metal burnups ranging from 1.0 to 15.8% FIMA. These conditions far exceeded the LHTGR peak design conditions of 8.0 x $10^{25}$ $n/m^2$ and 7.5% FIMA which were predicted at the time of the irradiation. The wide range of irradiation conditions was necessary to assess the differences in irradiation performance of the coating designs tested and to achieve high failure probabilities in some of the particle batches. This type of data is necessary for comparison of fuel particle behavior with performance models which are used to define the fertile particle design basis.

The results of the postirradiation examination of the GA fuel specimens are presented in this report. The results of the postirradiation examination of the ORNL fuel specimens and a more detailed description of the operation of the capsules is presented in Ref. 1.

# 2. DESCRIPTION OF EXPERIMENTS

## 2.1. OBJECTIVES

The specific objectives of this series of HT irradiation experiments are summarized as follows:

1. Evaluate the irradiation performance of BISO coated $ThO_2$ particles as a function of coating parameters, e.g., coating thickness, OPyC density, coating rate, and anisotropy.

2. Evaluate BISO particle dimensional change as a function of fast neutron exposure and heavy metal burnup.

3. Evaluate the irradiation performance of TRISO coated $ThO_2$ particles to provide guidance for further design improvements.

4. Provide particle samples for postirradiation annealing experiments designed to evaluate high-temperature survival rates, fission product retention, and fuel kernel migration.

## 2.2. DESCRIPTION OF FUEL SPECIMENS

The $ThO_2$ fuel kernels were fabricated by ORNL using the sol-gel process and were nominally 400 or 500 μm in diameter. The buffer and OPyC coatings were deposited at GA in a 5-in.-diameter coater from acetylene and propylene gases, respectively. Samples from 13 parent batches of BISO particles were tested. One batch of TRISO coated $ThO_2$ particles was also tested in the HT-17 through HT-19 series. A summary description of the parent particle batches is given in Table 1. Representative preirradiation

TABLE 1
SUMMARY DESCRIPTION OF PARTICLES TESTED IN CAPSULES HT-12 THROUGH HT-15 AND HT-17 THROUGH HT-19

| Batch Number | Kernel | | Buffer | | IPyC | | SiC | | OPyC | | | | Total Particle | |
|---|---|---|---|---|---|---|---|---|---|---|---|---|---|---|
| | Diameter (μm) | Density ($Mg/m^3$) | Thickness (μm) | Density ($Mg/m^3$) | Thickness (μm) | Density ($Mg/m^3$) | Thickness (μm) | Density ($Mg/m^3$) | Thickness (μm) | Density ($Mg/m^3$) | OPTAF[a] | Coating Rate (μm/min) | Diameter (μm) | Density ($Mg/m^3$) |
| 4252-00-013 | 405(±9)[b] | 9.9 | 81(±6) | 1.26 | -- | -- | -- | -- | 76(±6) | 2.00 | 1.14 | 2.4 | 717(±17) | 3.30 |
| 4252-01-071 | 495(±11) | 9.9 | 64(±6) | 1.11 | -- | -- | -- | -- | 75(±5) | 2.02 | 1.16 | 1.5-1.8 | 774(±19) | 4.07 |
| 4252-02-015 | 508(±10) | 10.0 | 83(±7) | 1.08 | -- | -- | -- | -- | 75(±8) | 1.84 | 1.07 | 4.1 | 825(±19) | 3.58 |
| 4252-03-012 | 501(±14) | 9.9 | 92(±10) | 1.00 | -- | -- | -- | -- | 67(±6) | 2.00 | >1.5 | 0.7 | 820(±25) | 3.60 |
| 4252-06-012 | 514(±9) | 9.9 | 80(±6) | 1.10 | -- | -- | -- | -- | 74(±6) | 1.82 | 1.14 | 5.6 | 819(±20) | 3.81 |
| 4252-07-016 | 485(±22) | 9.9 | 46(±5) | 1.03 | -- | -- | -- | -- | 50(±4) | 1.96 | 1.20 | 1.4 | 677(±19) | 4.84 |
| 4252-08-014 | 499(±17) | 10.0 | 39(±6) | 1.08 | -- | -- | -- | -- | 119(±11) | 1.95 | 1.14 | 1.3 | 821(±32) | 3.84 |
| 6542-01-013 | 500(±10) | 10.0 | 81(±9) | 1.08 | -- | -- | -- | -- | 87(±9) | 1.80 | 1.06 | 10.2 | 819(±43) | 3.44 |
| 6542-01-023 | 497(±12) | 9.8 | 80(±6) | 1.17 | -- | -- | -- | -- | 77(±6) | 1.82 | 1.10 | 2.8 | 807(±21) | 3.54 |
| 6542-02-023 | 470(±20) | 10.0 | 82(±8) | 1.08 | -- | -- | -- | -- | 78(±9) | 1.91 | 1.06 | 9.2 | 788(±35) | 3.45 |
| 6542-02-033 | 465(±17) | 9.8 | 73(±9) | 1.18 | -- | -- | -- | -- | 80(±8) | 1.89 | 1.12 | 2.3 | 765(±32) | 3.54 |
| 6542-16-013 | 493(±12) | 9.8 | 44(±5) | 1.08 | -- | -- | -- | -- | 57(±6) | 1.81 | 1.07 | 3.8 | 693(±17) | 4.78 |
| 6542-17-013 | 493(±11) | 9.8 | 47(±7) | 0.95 | -- | -- | -- | -- | 116(±12) | 1.86 | 1.27 | 2.7 | 814(±28) | 3.58 |
| 6252-01-023[c] | 458(±19) | 9.8 | 95(±16) | 1.26 | 28(±4) | 1.91 | 29(±5) | 3.21 | 36(±4) | 1.80 | 1.08 | 3.6 | 858(±36) | 3.28 |

[a] Optical anisotropy factor, relative units.

[b] Numbers in parentheses are standard deviations.

[c] TRISO particle batch.

photomicrographs of each particle batch are shown in Figs. A-1 through A-14 of the Appendix.

The particle batches were chosen so that only one variable (i.e., coating density, coating rate, or thickness) was tested at a time. To aid in postirradiation analysis the particles were selected so that the particles within each individual sample had a constant total coated particle density and a narrow distribution of kernel and total coated particle diameters. The steps used to separate desired particles from their respective parent batches are outlined in Fig. 1. Briefly, coated particles were sieved to plus or minus one standard deviation in particle diameter. They were then further separated by selecting, via constant density columns, only those particles having the batch-average total coated particle density. Following density separation, particles were individually radiographed and picked so that both kernel and total particle diameters were within 20 μm of their respective average values. As a final step, particles were heated in vacuum for 1 h at 1350°C to ensure volatilization of any of the fluids used for density separation.

## 2.3. CAPSULE DESIGN

The HT capsule, shown in Fig. 2, consisted of an aluminum tube with an external configuration identical to that of an HFIR target rod (Ref. 1). The capsule was sealed; therefore, there was no thermocouple instrumentation or utilization of a purge gas to monitor fission product activity. It was not possible to adjust fuel specimen temperatures in-pile.

Each capsule contained four cylindrical graphite magazines. Each magazine in turn contained 13 small graphite crucibles with an annular cavity which held 41 to 75 coated particles. Two of the magazines were designed to develop a 900°C temperature in the particle crucible and the other two a 1250°C crucible temperature. Only eight crucibles in each magazine contained test specimens. The remaining five crucibles contained low-enriched $UO_2$ particles which produced a more uniform power generation and specimen temperature over the life of the experiment.

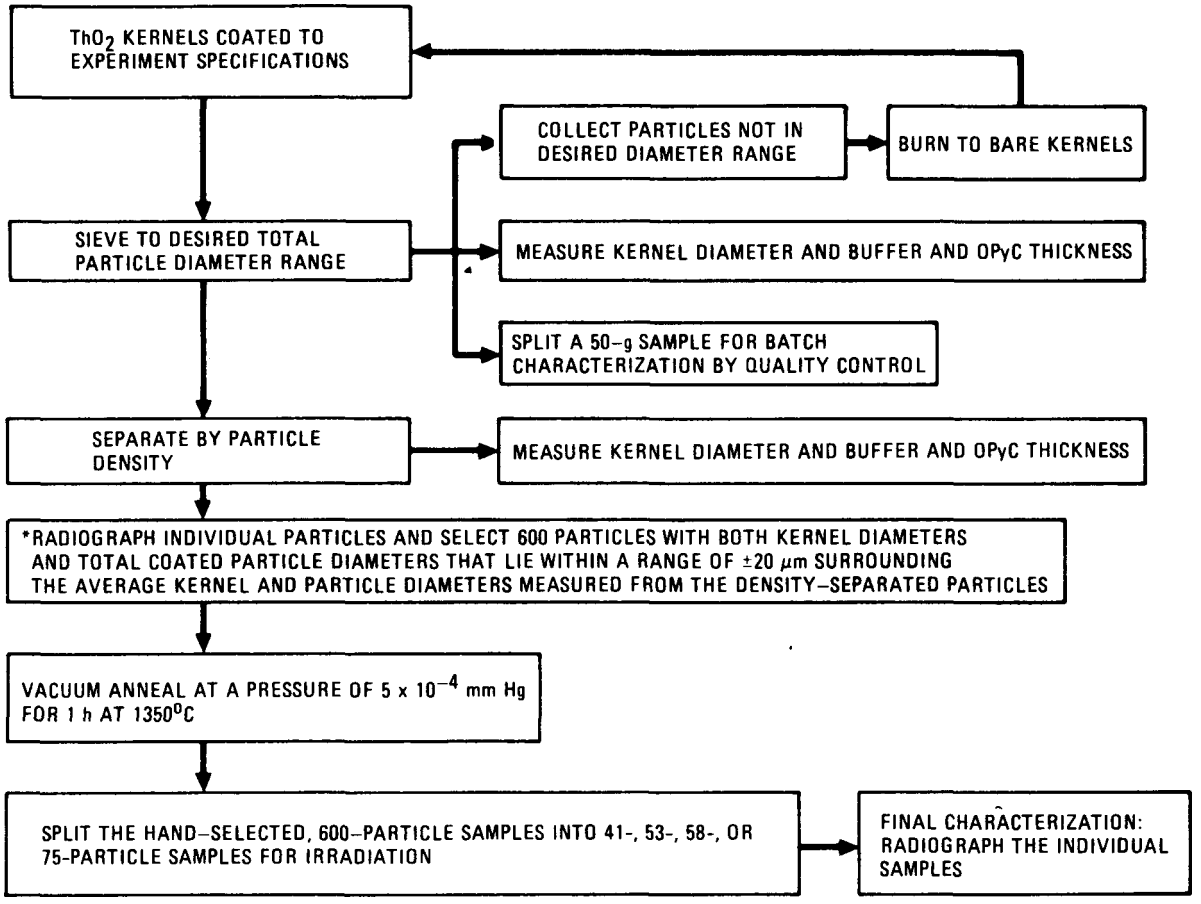


Fig. 1. Steps involved in selecting BISO coated $ThO_2$ particles for insertion in irradiation experiments HT-12 through HT-15 and HT-17 through HT-19

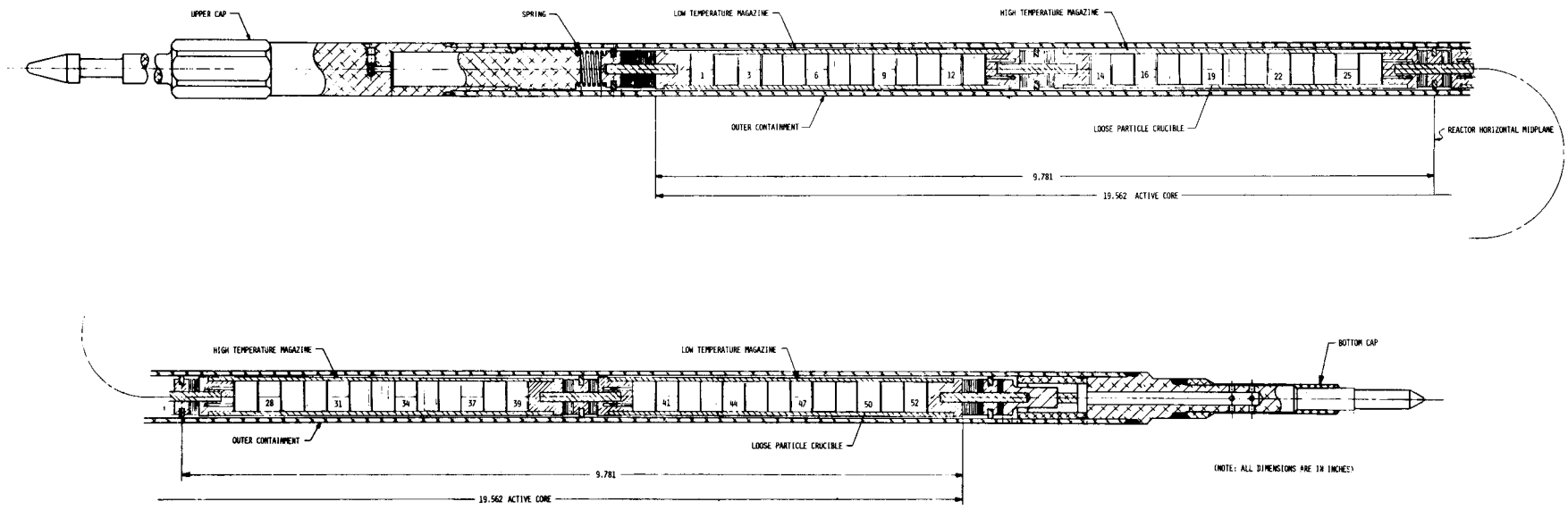


Fig. 2. Schematic showing the HT capsule design

# 3. IRRADIATION PARAMETERS

## 3.1. CAPSULE OPERATING HISTORY

The HFIR operating history for the cycles encompassing the periods of capsule irradiation is given in Table 2. All capsules completed their scheduled irradiation without any problems, with the exception of capsule HT-15. This capsule was withdrawn after seven cycles of irradiation, instead of the scheduled eight cycles, because extreme swelling of the Poco graphite magazines and crucibles was observed in capsule HT-14 after a six-cycle irradiation (Ref. 1).

## 3.2. NEUTRON FLUX CALCULATIONS

The fast neutron flux and fluence levels $(E > 29\ fJ)_{HFIR}$ were calculated by workers at ORNL and reported in Refs. 1 and 2. However, the flux spectrum in the HFIR differs somewhat from the design flux spectrum in an HTGR. An equivalent fast neutron fluence in an HTGR environment $(E > 29\ fJ)_{HTGR}$ was calculated for each fuel sample using Eq. 1 below (from Ref. 3) and these values are used in this report.

$$\phi_{HTGR} = 0.9\ \phi_{HFIR}\ (E > 29\ fJ) \qquad (1)$$

## 3.3. HEAVY METAL BURNUP CALCULATIONS

The heavy metal burnup was calculated for each fuel sample by workers at ORNL and the results were reported in Refs. 1 and 2. In these calculations it was assumed that all the Pa-233 formed from Th-232 decayed to U-233. However, some of the Pa-233 will capture a neutron to form Pa-234 and then decay to U-234, bypassing U-233, as shown in the Th-232 heavy metal fission chain below.

TABLE 2
OPERATIONAL HISTORY OF CAPSULES HT-12 THROUGH HT-15 AND HT-17 THROUGH HT-19

| Capsule | HFIR Cycle | Dates | | Operation (days) | Accumulated Irradiation Time at 100-MW Reactor Power (days) |
|---|---|---|---|---|---|
| | | Begin | End | | |
| HT-12 | 82 | 9/10/72 | 10/3/72 | 23 | 23.44 |
| | 83 | 10/8/72 | 10/23/72 | 15 | 38.62 |
| HT-13 | 83 | 10/8/72 | 10/23/72 | 15 | 15.18 |
| | 84A | 10/24/72 | 11/11/72 | 18 | |
| | 84B | 11/13/72 | 11/19/72 | 5 | 38.55 |
| | 85 | 11/20/72 | 12/13/72 | 23 | 74.14 |
| | 86(a) | 12/13/72 | 1/7/73 | 24 | 84.90 |
| | 87A | 1/9/73 | 1/10/73 | <1 | 85.50 |
| HT-14 | 85 | 11/20/72 | 12/13/72 | 23 | 23.09 |
| | 86(a) | 12/13/72 | 1/7/73 | 24 | 46.35 |
| | 87A | 1/9/73 | 1/10/73 | <1 | |
| | 87B | 1/12/73 | 2/3/73 | 21 | 68.86 |
| | 88 | 2/3/73 | 2/26/73 | 23 | 91.41 |
| | 89 | 2/27/73 | 3/22/73 | 23 | 114.14 |
| | 90 | 3/23/73 | 4/15/73 | 23 | 137.00 |
| HT-15 | 85 | 11/20/72 | 12/13/72 | 23 | 23.09 |
| | 86(a) | 12/13/72 | 1/7/73 | 24 | 46.35 |
| | 87A | 1/9/73 | 1/10/73 | <1 | |
| | 87B | 1/12/73 | 2/3/73 | 21 | 68.86 |
| | 88 | 2/3/73 | 2/26/73 | 23 | 91.41 |
| | 89 | 2/27/73 | 3/22/73 | 23 | 114.14 |
| | 90 | 3/23/73 | 4/15/73 | 23 | 137.00 |
| | 91 | 4/18/73 | 5/11/73 | 23 | 159.96 |
| HT-17 | 95 | 7/22/73 | 8/15/73 | 23 | 23.20 |
| | 96 | 8/16/73 | 9/8/73 | 23 | 46.42 |
| HT-18 | 95 | 7/22/73 | 8/15/73 | 23 | 23.20 |
| | 96 | 8/16/73 | 9/8/73 | 23 | 46.42 |
| | 97A(b) | 9/9/73 | 9/17/73 | | |
| | 97B | 9/17/73 | 10/5/73 | 26 | 69.58 |
| | 98 | 10/5/73 | 10/28/73 | 23 | 92.94 |
| HT-19 | 95 | 7/22/73 | 8/15/73 | 23 | 23.20 |
| | 96 | 8/16/73 | 9/8/73 | 23 | 46.42 |
| | 97A(b) | 9/9/73 | 9/17/73 | | |
| | 97B | 9/17/73 | 10/5/73 | 26 | 69.58 |
| | 98 | 10/5/73 | 10/28/73 | 23 | 92.94 |
| | 99 | 10/31/73 | 11/23/73 | 23 | 116.23 |
| | 100 | 11/25/73 | 12/17/73 | 23 | 139.27 |

(a) Includes two days at 50 MW.

(b) Reactor began a programmed reduction in power on 9/14/73 in preparation for the shutdown on 9/17/73.

Th-232 Series

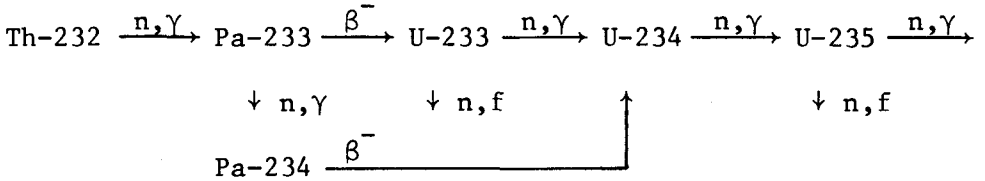


The heavy metal burnup for each sample was recalculated at GA using the FISSIN computer code (Ref. 4) to solve the above Th-232 transformation series. The reactor operating history given in Table 2 and the effective cross sections ($\bar{\sigma}$) given in Table 3 were used in these calculations.

Table 3
EFFECTIVE CROSS SECTIONS

| NUCLIDE | REACTION | $\bar{\sigma}$ (BARNS) |
|---|---|---|
| U-235 | (n,γ) | 76.6 |
| U-235 | (n,f) | 410.4 |
| Th-232 | (n,γ) | 8.3 |
| Pa-233 | (n,γ) | 70.6 |
| U-233 | (n,γ) | 41.2 |
| U-233 | (n,f) | 410.3 |
| U-234 | (n,γ) | 92.5 |
| U-236 | (n,γ) | 30.0 |
| U-238 | (n,γ) | 30.0 |

The more precisely calculated burnups were from 0 to ∿20% less than the burnups reported in Refs. 1 and 2. The burnups calculated using the FISSIN code were used in this report.

## 3.4. THERMAL ANALYSIS

There were no provisions for direct temperature monitoring in the HT capsules. A detailed thermal analysis of each capsule was performed by ORNL with the HTCAP computer code (Ref. 5). The total heat generation

within each capsule was calculated, and a modified one-dimensional heat transfer analysis was performed. The maximum particle surface operating temperatures and graphite specimen holder temperatures were calculated at 1-day intervals for each HFIR irradiation cycle. The time-averaged particle surface temperature for each fuel sample is reported in Tables 4 through 11.

Graphite specimen holder design temperatures were 1250°C for the high-flux regions and 900°C for the low-flux regions. The calculated irradiation temperature and power generated per particle for representative low-temperature and high-temperature specimens are plotted in Figs. 3 and 4,* respectively. In general, the graphite specimen holders operated between 50° and 200°C higher than the original design temperature, depending on their location in a particular sleeve. The maximum particle surface temperatures exceeded specimen holder temperatures by as much as 100°C after one cycle and peaked at approximately 300°C higher during the fourth cycle in the high-temperature regions and the sixth cycle in the low-temperature regions.

---

*Courtesy of M. J. Kania, Metals and Ceramics Division, Oak Ridge National Laboratory.

TABLE 4
IRRADIATION CONDITIONS AND RESULTS OF $ThO_2$ BISO PARTICLES IRRADIATED IN CAPSULE HT-12

| Particle Description | | | | | | Holder No. | Irradiation Conditions | | | Number of Particles Tested | OPyC Failure[f] (%) | Postirradiation Examinations Performed | | |
|---|---|---|---|---|---|---|---|---|---|---|---|---|---|---|
| | | | Outer Pyrocarbon (OPyC) | | | | Time-Averaged Temp[d] (°C) | Fast Fluence ($10^{25}$ n/m$^2$) (E > 29 fJ)$_{HTGR}$ | Burnup[e] (% FIMA) | | | Particle Density[c] | Metallography | X-ray Radiography |
| Batch No. | Kernel Diameter[a] (μm) | Buffer Thickness[a] (μm) | Thickness[a] (μm) | Density[b,c] (Mg/m$^3$) | Coating Rate (μm/min) | | | | | | | | | |
| 4252-00-013-3 | 404 | 77 | 79 | 2.00 | 2.3 | 20 | 1325 | 3.4 | 1.8 | 75 | 3 | X | | X |
| 4252-00-013-7 | 397 | 79 | 79 | 2.00 | 2.3 | 7 | 1025 | 2.2 | 1.3 | 53 | 0 | X | | X |
| 4252-01-071-3 | 494 | 62 | 75 | 2.02 | 1.6 | 33 | 1390 | 3.4 | 1.8 | 75 | 33 | | | |
| 4252-01-071-7 | 491 | 62 | 73 | 2.02 | 1.6 | 46 | 1115 | 2.2 | 1.3 | 53 | 0 | | | |
| 4252-02-015-1 | 510 | 86 | 70 | 1.84 | 3.9 | 27 | 1445 | 3.5 | 1.9 | 75 | 0 | | | |
| 4252-02-015-5 | 505 | 85 | 76 | 1.84 | 4.2 | 40 | 1170 | 2.8 | 1.5 | 53 | 0 | X | X | X |
| 4252-03-012-1 | 503 | 86 | 70 | 2.00 | 0.7 | 30 | 1400 | 3.5 | 1.9 | 75 | 100 | | | |
| 4252-03-012-5 | 505 | 92 | 68 | 2.00 | 0.7 | 43 | 1110 | 2.5 | 1.4 | 53 | 0 | | | |
| 4252-06-012-1 | 513 | 78 | 74 | 1.82 | 5.6 | 23 | 1410 | 3.5 | 1.9 | 75 | 0 | X | | X |
| 4252-06-012-5 | 515 | 76 | 78 | 1.82 | 5.9 | 10 | 1120 | 2.5 | 1.4 | 53 | 2 | X | | X |
| 4252-07-016-1 | 491 | 45 | 48 | 1.96 | 1.3 | 36 | 1400 | 3.2 | 1.8 | 75 | 27 | | | |
| 4252-07-016-5 | 492 | 45 | 51 | 1.96 | 1.4 | 49 | 1090 | 2.0 | 1.1 | 53 | 0 | | | X |
| 4252-08-014-1 | 488 | 39[b] | 119[b] | 1.95 | 1.3[b] | 15 | 1460 | 3.2 | 1.7 | 75 | 59 | | | |
| 4252-08-014-5 | 494 | 39[b] | 119[b] | 1.95 | 1.3[b] | 2 | 1185 | 1.8 | 1.0 | 53 | 0 | X | | X |

[a] Measured on particle sample that was irradiated.

[b] Measured on parent particle batch.

[c] Measured using density gradient column.

[d] Time-averaged maximum particle surface temperatures; average kernel temperatures are 35° to 65°C higher than surface temperatures.

[e] Calculated at GA using FISSIN computer code.

[f] Determined during visual examination.

TABLE 5
IRRADIATION CONDITIONS AND RESULTS OF $ThO_2$ BISO PARTICLES IRRADIATED IN CAPSULE HT-13

| Particle Description | | | | | | Holder No. | Irradiation Conditions | | | Number of Particles Tested | OPyC Failure[f] (%) | Postirradiation Examinations Performed | | |
|---|---|---|---|---|---|---|---|---|---|---|---|---|---|---|
| | | | Outer Pyrocarbon (OPyC) | | | | Time-Averaged Temp[d] (°C) | Fast Fluence ($10^{25}$ n/m$^2$) (E > 29 fJ)$_{HTGR}$ | Burnup[e] (% FIMA) | | | Particle Density[c] | Metallography | X-ray Radiography |
| Batch No. | Kernel Diameter[a] (μm) | Buffer Thickness[a] (μm) | Thickness[a] (μm) | Density[b,c] (Mg/m$^3$) | Coating Rate (μm/min) | | | | | | | | | |
| 4252-00-013-4 | 406 | 81 | 79 | 2.00 | 2.3 | 20 | 1390 | 7.5 | 6.7 | 75 | 100 | | | |
| 4252-00-013-8 | 404 | 78 | 80 | 2.00 | 2.4 | 7 | 1100 | 5.0 | 5.0 | 53 | 8 | X | | X |
| 4252-01-071-4 | 494 | 65 | 73 | 2.02 | 1.6 | 33 | 1485 | 7.5 | 6.7 | 75 | 100 | | | |
| 4252-01-071-8 | 496 | 60 | 77 | 2.02 | 1.6 | 46 | 1210 | 5.0 | 5.0 | 53 | 34 | | | |
| 4252-02-015-2 | 502 | 89 | 67 | 1.84 | 3.7 | 27 | 1515 | 7.7 | 6.9 | 75 | 88 | | | |
| 4252-02-015-6 | 508 | 84 | 75 | 1.84 | 4.1 | 40 | 1255 | 6.2 | 5.8 | 53 | 0 | X | X | X |
| 4252-03-012-2 | 498 | 95 | 64 | 2.00 | 0.6 | 30 | 1490 | 7.6 | 6.8 | 75 | 100 | | | |
| 4252-03-012-6 | 505 | 92 | 66 | 2.00 | 0.7 | 43 | 1215 | 5.6 | 5.5 | 53 | 100 | | | |
| 4252-06-012-2 | 517 | 79 | 77 | 1.82 | 5.8 | 23 | 1510 | 7.6 | 6.8 | 75 | 80 | | | |
| 4252-06-012-6 | 517 | 78 | 74 | 1.82 | 5.8 | 10 | 1230 | 5.6 | 5.5 | 53 | 0 | X | | X |
| 4252-07-016-2 | 483 | 42 | 48 | 1.96 | 1.3 | 36 | 1505 | 7.3 | 6.5 | 75 | 100 | | | |
| 4252-07-016-6 | 492 | 45 | 50 | 1.96 | 1.4 | 49 | 1200 | 4.4 | 4.6 | 53 | 42 | | | X |
| 4252-08-014-2 | 465 | 39[b] | 119[b] | 1.95 | 1.3[b] | 15 | 1535 | 7.0 | 6.4 | 75 | 100 | | | |
| 4252-08-014-6 | 484 | 39[b] | 119[b] | 1.95 | 1.3[b] | 2 | 1255 | 3.9 | 4.1 | 53 | 94 | | | |

[a] Measured on particle sample that was irradiated.

[b] Measured on parent particle batch.

[c] Measured using density gradient column.

[d] Time-averaged maximum particle surface temperatures; average kernel temperatures are 35° to 65°C higher than surface temperatures.

[e] Calculated at GA using FISSIN computer code.

[f] Determined during visual examination.

TABLE 6
IRRADIATION CONDITIONS AND RESULTS OF $ThO_2$ BISO PARTICLES IRRADIATED IN CAPSULE HT-14

| Particle Description | | | | | | Holder No. | Irradiation Conditions | | | Number of Particles Tested | OPyC Failure[f] (%) | Postirradiation Examinations Performed | | |
|---|---|---|---|---|---|---|---|---|---|---|---|---|---|---|
| | | | Outer Pyrocarbon (OPyC) | | | | Time-Averaged Temp[d] (°C) | Fast Fluence ($10^{25}$ n/m$^2$) (E > 29 fJ)$_{HTGR}$ | Burnup[e] (% FIMA) | | | Particle Density[c] | Metallography | X-ray Radiography |
| Batch No. | Kernel Diameter[a] (μm) | Buffer Thickness[a] (μm) | Thickness[a] (μm) | Density[b,c] (Mg/m$^3$) | Coating Rate (μm/min) | | | | | | | | | |
| 4252-00-013-5 | 403 | 77 | 82 | 2.00 | 2.4 | 20 | 1425 | 12.1 | 13.0 | 75 | 100[g] | | | |
| 4252-00-013-9 | 404 | 78 | 81 | 2.00 | 2.4 | 7 | 1145 | 8.1 | 10.0 | 53 | 98 | | | |
| 4252-01-071-5 | 494 | 62 | 75 | 2.02 | 1.6 | 33 | 1530 | 12.1 | 13.0 | 75 | 100[g] | | | |
| 4252-01-071-9 | 495 | 64 | 73 | 2.02 | 1.6 | 46 | 1265 | 8.1 | 10.0 | 53 | 100 | | | |
| 4252-02-015-3 | 508 | 85 | 74 | 1.84 | 4.1 | 27 | 1545 | 12.5 | 13.3 | 75 | 90 | | | |
| 4252-02-015-7 | 509 | 88 | 68 | 1.84 | 3.8 | 40 | 1305 | 9.9 | 11.4 | 53 | 0 | X | X | X |
| 4252-03-012-3 | 499 | 90 | 72 | 2.00 | 0.7 | 30 | 1540 | 12.3 | 13.1 | 75 | 100[g] | | | |
| 4252-03-012-7 | 501 | 95 | 63 | 2.00 | 0.6 | 43 | 1270 | 9.0 | 10.8 | 53 | 100 | | | |
| 4252-06-012-3 | 515 | 76 | 79 | 1.82 | 6.0 | 23 | 1556 | 12.3 | 13.1 | 75 | 85 | | | |
| 4252-06-012-7 | 513 | 80 | 75 | 1.82 | 5.7 | 10 | 1290 | 9.0 | 10.8 | 53 | 0 | X | X | X |
| 4252-07-016-3 | 490 | 46 | 47 | 1.96 | 1.3 | 36 | 1555 | 11.6 | 12.6 | 75 | 100[g] | | | |
| 4252-07-016-7 | 487 | 44 | 48 | 1.96 | 1.3 | 49 | 1260 | 7.1 | 9.1 | 53 | 98 | | | |
| 4252-08-014-3 | 461 | 39[b] | 119[b] | 1.95 | 1.3[b] | 15 | 1570 | 11.2 | 12.4 | 75 | 100[g] | | | |
| 4252-08-014-7 | 492 | 39[b] | 119[b] | 1.95 | 1.3[b] | 2 | 1305 | 6.2 | 8.3 | 53 | 100 | | | |

[a] Measured on particle sample that was irradiated.

[b] Measured on parent particle batch.

[c] Measured using density gradient column.

[d] Time-averaged maximum particle surface temperatures; average kernel temperatures are 50° to 95°C higher than surface temperatures.

[e] Calculated at GA using FISSIN computer code.

[f] Determined during visual examination.

[g] Sample not examined. 100% failure assumed based on HT-13 irradiation results.

TABLE 7
IRRADIATION CONDITIONS AND RESULTS OF $ThO_2$ BISO PARTICLES IRRADIATED IN CAPSULE HT-15

| Particle Description | | | | | | | Irradiation Conditions | | | | | Postirradiation Examinations Performed | | |
|---|---|---|---|---|---|---|---|---|---|---|---|---|---|---|
| | | | Outer Pyrocarbon (OPyC) | | | | | | | | | | | |
| Batch No. | Kernel Diameter[a] (μm) | Buffer Thickness[a] (μm) | Thickness[a] (μm) | Density[b,c] ($Mg/m^3$) | Coating Rate (μm/min) | Holder No. | Time Average Temp[d] (°C) | Fast Fluence ($10^{25}$ $n/m^2$) ($E > 29$ fJ)$_{HTGR}$ | Burnup[e] (% FIMA) | Number of Particles Tested | OPyC Failure[f] (%) | Particle Density[c] | Metallography | X-ray Radiography |
| 4252-00-013-6 | 404 | 78 | 77 | 2.00 | 2.3 | 20 | 1430 | 14.0 | 15.7 | 75 | 100[g] | | | |
| 4252-00-013-10 | 393 | 78 | 79 | 2.00 | 2.3 | 7 | 1155 | 9.4 | 12.2 | 53 | 87 | | | |
| 4252-01-071-6 | 495 | 61 | 74 | 2.02 | 1.6 | 33 | 1541 | 14.0 | 15.7 | 75 | 100[g] | | | |
| 4252-01-071-10 | 494 | 63 | 76 | 2.02 | 1.7 | 46 | 1285 | 9.4 | 12.2 | 53 | 98 | | | |
| 4252-02-015-4 | 510 | 86 | 69 | 1.84 | 3.8 | 27 | 1552 | 14.6 | 16.1 | 75 | 91 | | | |
| 4252-02-015-8 | 509 | 86 | 75 | 1.84 | 4.1 | 40 | 1315 | 11.5 | 13.8 | 53 | 45 | X | X | X |
| 4252-03-012-4 | 505 | 90 | 71 | 2.00 | 0.7 | 30 | 1545 | 14.4 | 15.8 | 75 | 100[g] | | | |
| 4252-03-012-8 | 503 | 96 | 64 | 2.00 | 0.6 | 43 | 1285 | 10.5 | 13.3 | 53 | 100[g] | | | |
| 4252-06-012-4 | 515 | 76 | 78 | 1.82 | 5.9 | 23 | 1565 | 14.4 | 15.8 | 75 | 82 | | | |
| 4252-06-012-8 | 509 | 77 | 75 | 1.82 | 5.6 | 10 | 1305 | 10.5 | 13.3 | 53 | 0 | X | | X |
| 4252-07-016-4 | 492 | 45 | 51 | 1.96 | 1.4 | 36 | 1565 | 13.6 | 15.3 | 75 | 100 | | | |
| 4252-07-016-8 | 494 | 46 | 48 | 1.96 | 1.3 | 49 | 1280 | 8.4 | 11.3 | 53 | 100[g] | | | |
| 4252-08-014-4 | 504 | 39[b] | 119[b] | 1.95 | 1.3[b] | 15 | 1580 | 13.1 | 15.0 | 75 | 100[g] | | | |
| 4252-08-014-8 | 503 | 39[b] | 119[b] | 1.95 | 1.3[b] | 2 | 1315 | 7.3 | 10.3 | 53 | 100[g] | | | |

[a] Measured on particle sample that was irradiated.

[b] Measured on parent particle batch.

[c] Measured using density gradient column.

[d] Time-averaged maximum particle surface temperatures; average kernel temperatures are 50° to 95°C higher than surface temperatures.

[e] Calculated at GA using FISSIN computer code.

[f] Determined during visual examination.

[g] Sample not examined. 100% failure assumed based on HT-13 and HT-14 irradiation results.

TABLE 8
IRRADIATION CONDITIONS AND RESULTS OF $ThO_2$ BISO PARTICLES IRRADIATED IN CAPSULE HT-17

| Particle Description | | | | | | | Irradiation Conditions | | | | | Postirradiation Examinations Performed | |
|---|---|---|---|---|---|---|---|---|---|---|---|---|---|
| | | | Outer Pyrocarbon (OPyC) | | | | | | | | | | |
| Batch No. | Kernel Diameter[a] (μm) | Buffer Thickness[a] (μm) | Thickness[a] (μm) | Density[b,c] ($Mg/m^3$) | Coating Rate (μm/min) | Holder No. | Time-Averaged Temp[d] (°C) | Fast Fluence ($10^{25}$ n/$m^2$) (E > 29 fJ)$_{HTGR}$ | Burnup[e] (% FIMA) | Number of Particles Tested | OPyC Failure[f] (%) | Particle Density[c] | X-ray Radiography |
| 6542-01-013-7 | 509 | 79 | 89 | 1.82 | 10.5 | 40 | 1170 | 3.3 | 2.0 | 41 | 0 | X | X |
| 6542-01-013-10 | 512 | 79 | 91 | 1.82 | 10.7 | 27 | 1435 | 4.2 | 2.4 | 58 | 0 | X | X |
| 6542-01-023-1 | 490 | 79 | 73 | 1.83 | 2.7 | 42 | 1140 | 3.2 | 1.9 | 41 | 0 | X | X |
| 6542-01-023-4 | 483 | 79 | 70 | 1.83 | 2.6 | 29 | 1415 | 4.2 | 2.4 | 58 | 0 | X | X |
| 6542-02-023-1 | 475 | 85 | 71 | 1.94 | 8.4 | 43 | 1115 | 3.1 | 1.9 | 41 | 0 | X | X |
| 6542-02-023-4 | 477 | 87 | 70 | 1.94 | 8.2 | 30 | 1395 | 4.2 | 2.4 | 58 | 0 | X | X |
| 6542-02-033-1 | 471 | 74 | 67 | 1.88 | 2.0 | 45 | 1100 | 2.9 | 1.7 | 41 | 0 | X | X |
| 6542-02-033-4 | 471 | 77 | 72 | 1.88 | 2.1 | 32 | 1395 | 4.1 | 2.4 | 58 | 0 | X | X |
| 6542-16-013-1 | 484 | 48 | 52 | 1.81 | 3.5 | 46 | 1170 | 2.9 | 1.6 | 41 | 0 | | X |
| 6542-16-013-4 | 488 | 44 | 52 | 1.81 | 3.5 | 33 | 1445 | 4.1 | 2.4 | 58 | 2 | X | X |
| 6542-17-013-1 | 497 | 48 | 107 | 1.86 | 2.5 | 48 | 1105 | 2.5 | 1.5 | 41 | 0 | X | X |
| 6542-17-013-4 | 501 | 47 | 112 | 1.86 | 2.6 | 35 | 1390 | 4.0 | 2.3 | 58 | 0 | X | X |

[a] Measured on particle sample that was irradiated.

[b] Measured on parent particle batch.

[c] Measured using density gradient column.

[d] Time-averaged maximum particle surface temperatures; average kernel temperatures are 35° to 65°C higher than surface temperatures.

[e] Calculated at GA using FISSIN computer code.

[f] Determined during visual examination.

TABLE 9
IRRADIATION CONDITIONS AND RESULTS OF $ThO_2$ BISO PARTICLES IRRADIATED IN CAPSULE HT-18

| Particle Description | | | | | | Holder No. | Irradiation Conditions | | | Number of Particles Tested | OPyC Failure(f) (%) | Postirradiation Examinations Performed | |
|---|---|---|---|---|---|---|---|---|---|---|---|---|---|
| | | | Outer Pyrocarbon (OPyC) | | | | | | | | | | |
| Batch No. | Kernel Diameter(a) (μm) | Buffer Thickness(a) (μm) | Thickness(a) (μm) | Density(b,c) ($Mg/m^3$) | Coating Rate (μm/min) | | Time-Averaged Temp(d) (°C) | Fast Fluence ($10^{25}$ n/$m^2$) (E > 29 fJ)HTGR | Burnup(e) (% FIMA) | | | Particle Density(c) | X-ray Radiography |
| 6542-01-013-8 | 509 | 80 | 87 | 1.82 | 10.2 | 40 | 1250 | 6.8 | 6.6 | 41 | 2 | X | X |
| 6542-01-013-11 | 511 | 82 | 90 | 1.82 | 10.6 | 27 | 1500 | 8.6 | 7.9 | 58 | 9 | X | X |
| 6542-01-023-2 | 486 | 80 | 73 | 1.83 | 2.7 | 42 | 1245 | 6.4 | 6.5 | 41 | 46 | X | X |
| 6542-01-023-5 | 479 | 79 | 74 | 1.83 | 2.7 | 29 | 1505 | 8.5 | 7.8 | 58 | 2 | X | X |
| 6542-02-023-2 | 476 | 84 | 70 | 1.94 | 8.2 | 43 | 1215 | 6.1 | 6.3 | 41 | 15 | X | X |
| 6542-02-023-5 | 474 | 84 | 70 | 1.94 | 8.2 | 30 | 1485 | 8.5 | 7.7 | 58 | 0 | X | X |
| 6542-02-033-2 | 469 | 74 | 71 | 1.88 | 2.1 | 45 | 1200 | 5.8 | 5.9 | 41 | 24 | | |
| 6542-02-033-5 | 474 | 76 | 72 | 1.88 | 2.1 | 32 | 1485 | 8.3 | 7.7 | 58 | 74 | | |
| 6542-16-013-2 | 489 | 46 | 54 | 1.81 | 3.6 | 46 | 1280 | 5.5 | 5.7 | 41 | 17 | | X |
| 6542-16-013-5 | 481 | 47 | 53 | 1.81 | 3.5 | 33 | 1550 | 8.2 | 7.7 | 58 | 100 | | |
| 6542-17-013-2 | 497 | 45 | 110 | 1.86 | 2.6 | 48 | 1195 | 5.1 | 5.4 | 41 | 14 | X | X |
| 6542-17-013-5 | 500 | 46 | 108 | 1.86 | 2.5 | 35 | 1485 | 8.1 | 7.5 | 58 | 95 | | |

(a) Measured on particle sample that was irradiated.

(b) Measured on parent particle batch.

(c) Measured using density gradient column.

(d) Time-averaged maximum particle surface temperatures; average kernel temperatures are 50° to 95° higher than surface temperatures.

(e) Calculated at GA using FISSIN computer code.

(f) Determined during visual examination.

TABLE 10
IRRADIATION CONDITIONS AND RESULTS OF $ThO_2$ BISO PARTICLES IRRADIATED IN CAPSULE HT-19

| Particle Description | | | | | | | Irradiation Conditions | | | | | Postirradiation Examinations Performed | |
|---|---|---|---|---|---|---|---|---|---|---|---|---|---|
| | | | Outer Pyrocarbon (OPyC) | | | | | | | | | | |
| Batch No. | Kernel Diameter[a] (μm) | Buffer Thickness[a] (μm) | Thickness[a] (μm) | Density[b,c] ($Mg/m^3$) | Coating Rate (μm/min) | Holder No. | Time-Averaged Temp[d] (°C) | Fast Fluence ($10^{25}$ n/m$^2$) (E > 29 fJ)$_{HTGR}$ | Burnup[e] (% FIMA) | Number of Particles Tested | OPyC Failure[f] (%) | Density[c] | X-ray Radiography |
| 6542-01-013-9 | 511 | 81 | 90 | 1.82 | 10.6 | 40 | 1290 | 10.1 | 11.7 | 41 | 17 | X | X |
| 6542-01-013-12 | 510 | 80 | 89 | 1.82 | 10.5 | 27 | 1520 | 12.8 | 13.6 | 58 | 97 | | |
| 6542-01-023-3 | 490 | 81 | 69 | 1.83 | 2.5 | 42 | 1290 | 9.6 | 11.5 | 41 | 73 | | |
| 6542-01-023-6 | 480 | 79 | 72 | 1.83 | 2.6 | 29 | 1545 | 12.7 | 13.5 | 58 | 98 | | |
| 6542-02-023-3 | 472 | 87 | 68 | 1.94 | 8.0 | 43 | 1260 | 9.3 | 11.2 | 41 | 3 | X | X |
| 6542-02-023-6 | 474 | 85 | 71 | 1.94 | 8.4 | 30 | 1520 | 12.6 | 13.4 | 58 | 0 | X | X |
| 6542-02-033-3 | 471 | 77 | 72 | 1.88 | 2.1 | 45 | 1245 | 8.6 | 10.6 | 41 | 66 | | |
| 6542-02-033-6 | 468 | 76 | 72 | 1.88 | 2.1 | 32 | 1520 | 12.4 | 13.3 | 58 | 100 | | |
| 6542-16-013-3 | 481 | 46 | 52 | 1.81 | 3.5 | 46 | 1335 | 8.3 | 10.2 | 41 | 74 | | |
| 6542-16-013-6 | 483 | 45 | 55 | 1.81 | 3.7 | 33 | 1590 | 12.3 | 13.3 | 58 | 100 | | |
| 6542-17-013-3 | 500 | 45 | 113 | 1.86 | 2.6 | 48 | 1240 | 7.6 | 9.8 | 41 | 98 | | |
| 6542-17-013-6 | 497 | 44 | 115 | 1.86 | 2.7 | 35 | 1520 | 12.1 | 13.0 | 58 | 100 | | |

[a] Measured on particle sample that was irradiated.

[b] Measured on parent particle batch.

[c] Measured using density gradient column.

[d] Time-averaged maximum particle surface temperatures; average kernel temperatures are 50° to 95°C higher than surface temperatures.

[e] Calculated at GA using FISSIN computer code.

[f] Determined during visual examination.

TABLE 11
IRRADIATION CONDITIONS AND RESULTS OF $ThO_2$ TRISO PARTICLES IRRADIATED IN CAPSULES HT-17, -18, AND -19

| Batch No. | Particle Description | | | | | | Irradiation Conditions | | | | Postirradiation | | |
|---|---|---|---|---|---|---|---|---|---|---|---|---|---|
| | Kernel Diameter[a] (μm) | Coating Thickness (μm) | | | | Total Particle Diameter (μm) | Capsule Position | Time-Averaged Temp[c] (°C) | Fast Fluence ($10^{25}$ n/cm$^2$) (E > 29 fJ)$_{HTGR}$ | Burnup[d] (% FIMA) | Number of Particles Tested | OPyC Failure[e] (%) | Pressure Vessel Failure[e] (%) |
| | | Buffer[b] | IPyC[b] | SiC[a] | OPyC[a] | | | | | | | | |
| 6252-01-023-1 | 498 | 95 | 28 | 26 | 37 | 884 | HT-17-49 | 1055 | 2.4 | 1.5 | 41 | 56 | 0 |
| 6252-01-023-4 | 495 | 95 | 28 | 26 | 37 | 879 | HT-17-36 | 1365 | 4.0 | 2.3 | 58 | 78 | 53 |
| 6252-01-023-7 | 491 | 95 | 28 | 28 | 36 | 865 | HT-17-51 | 1070 | 2.2 | 1.3 | 41 | 83 | 0 |
| 6252-01-023-10 | 487 | 95 | 28 | 29 | 33 | 868 | HT-17-38 | 1410 | 3.9 | 2.2 | 58 | 74 | 50 |
| 6252-01-023-2 | 496 | 95 | 28 | 26 | 37 | 877 | HT-18-49 | 1145 | 4.9 | 5.2 | 41 | 83 | 66 |
| 6252-01-023-5 | 497 | 95 | 28 | 25 | 37 | 880 | HT-18-36 | 1450 | 7.9 | 7.4 | 58 | 86 | 79 |
| 6252-01-023-8 | 489 | 95 | 28 | 29 | 35 | 858 | HT-18-51 | 1130 | 4.2 | 4.7 | 41 | 61 | 7 |
| 6252-01-023-11 | 478 | 95 | 28 | 30 | 34 | 843 | HT-18-38 | 1460 | 7.6 | 7.3 | 58 | 86 | 81 |
| 6252-01-023-3 | 502 | 95 | 28 | 26 | 38 | 891 | HT-19-49 | 1185 | 7.4 | 9.4 | 41 | 88 | 80 |
| 6252-01-023-6 | 497 | 95 | 28 | 27 | 37 | 884 | HT-19-36 | 1485 | 11.9 | 12.9 | 58 | 85 | 71 |
| 6252-01-023-9 | 489 | 95 | 28 | 28 | 35 | 874 | HT-19-51 | 1160 | 6.4 | 8.6 | 41 | 74 | 58 |
| 6252-01-023-12 | 492 | 95 | 28 | 27 | 35 | 849 | HT-19-38 | 1480 | 11.5 | 12.7 | 58 | 86 | 81 |

[a] Measured on particle sample that was irradiated.

[b] Measured on parent particle batch.

[c] Time-averaged maximum particle surface temperatures; average kernel temperatures are 110° to 180°C higher than surface temperatures.

[d] Calculated at GA using FISSIN computer code.

[e] Determined during visual examination.

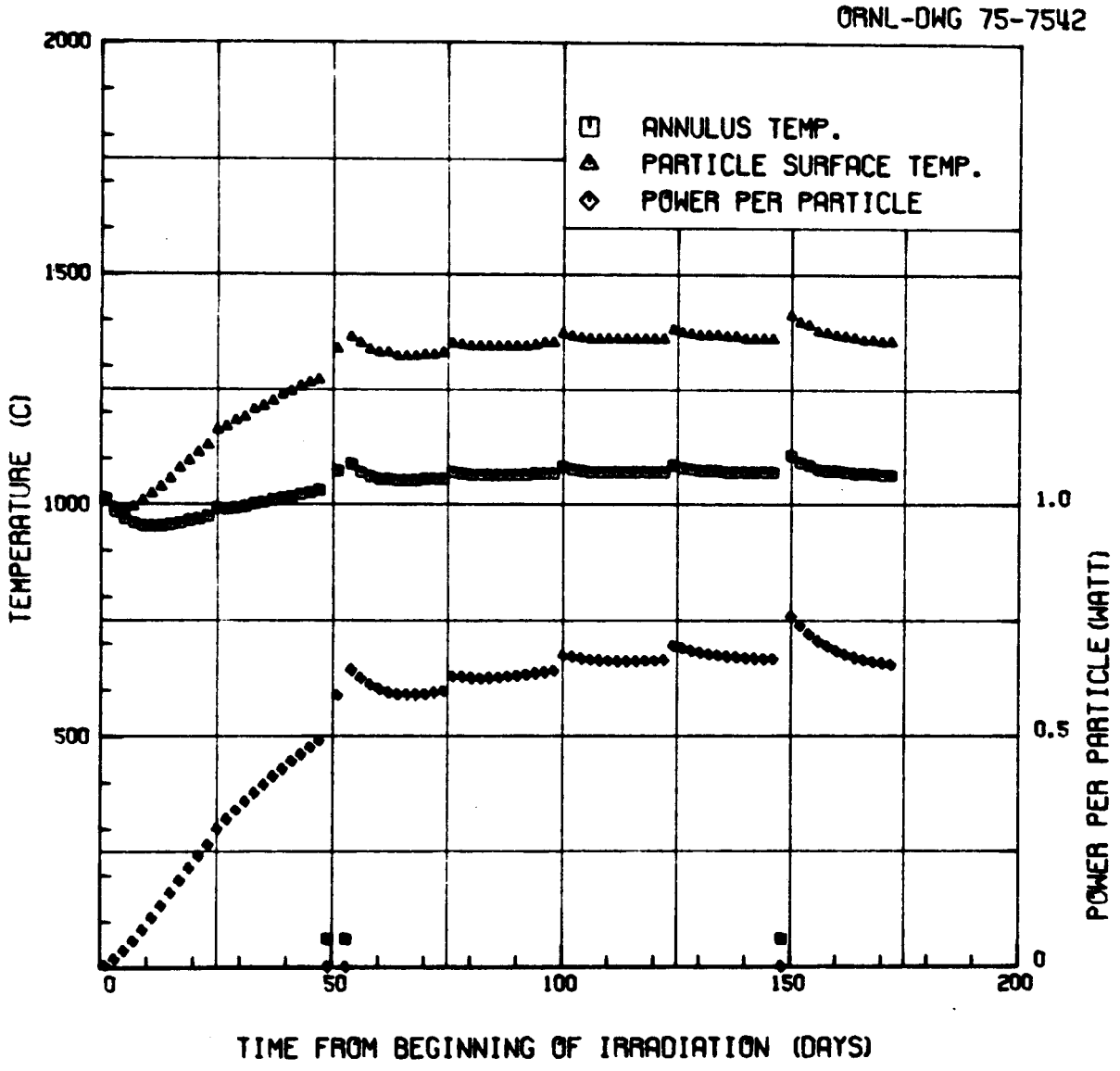


Fig. 3. Calculated irradiation temperature and power generated per particle in a representative low-temperature position (holder 43) of capsules HT-14 and HT-15

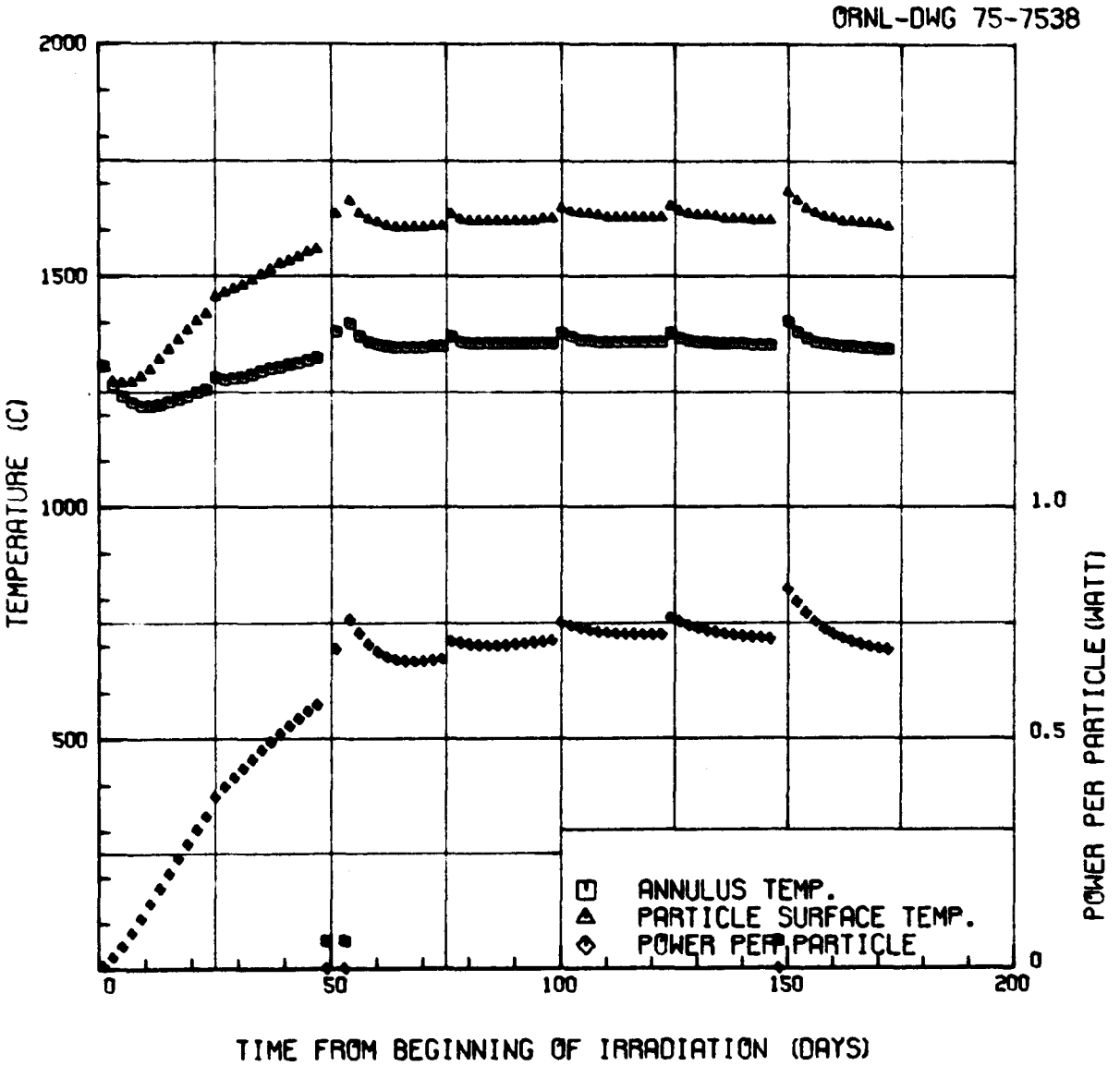


Fig. 4. Calculated irradiation temperature and power generated per particle in a representative high-temperature position (holder 36) of capsules HT-14 and HT-15

# 4. RESULTS OF POSTIRRADIATION EXAMINATIONS

Disassembly of the capsules and unloading of the fuel particles from their graphite holders were completed at ORNL (Ref. 1). After removal the fuel specimens were visually examined and photographed in-cell. The fuel specimens were then shipped to GA for additional postirradiation characterization. The samples were re-examined visually and particle density measurements, metallography, and X-ray radiography examinations were performed on selected fuel samples noted in Tables 4 through 11.

## 4.1. VISUAL EXAMINATION

The visual examination conducted at GA was performed using an in-cell stereomicroscope with a magnification range of 4X to 30X. Coating failure levels observed in the particle samples during this examination are reported in Tables 4 through 11. The majority of the fuel samples tested in the low-exposure capsules (HT-12 and HT-17) did not exhibit coating failure. As the irradiation conditions became more severe in the subsequent capsules, the coating failure levels increased in most of the particle samples as was expected. This was particularly evident in the particle batches having OPyC coatings deposited at low coating rates, as shown in Fig. 5.

Examination of some of the samples in the higher fluence HT-14 and HT-15 capsules was not considered warranted. A failure level of 100% was assigned to these samples based on the results obtained in the previous capsule.

The $ThO_2$ fuel kernels were intact in particle batches that experienced coating failure late in the irradiation. However, if the failure occurred

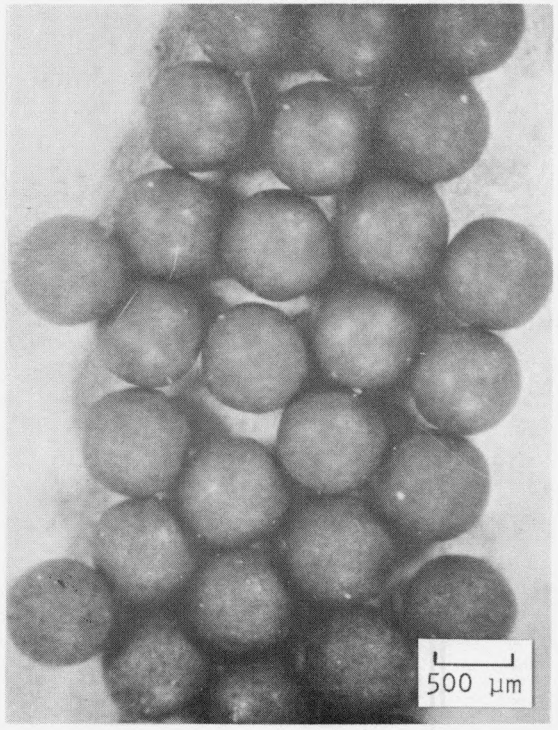


S7305-12

HT-12: 0% FAILURE
1090°C
2.0 X $10^{25}$ n/$m^2$
1.1% FIMA

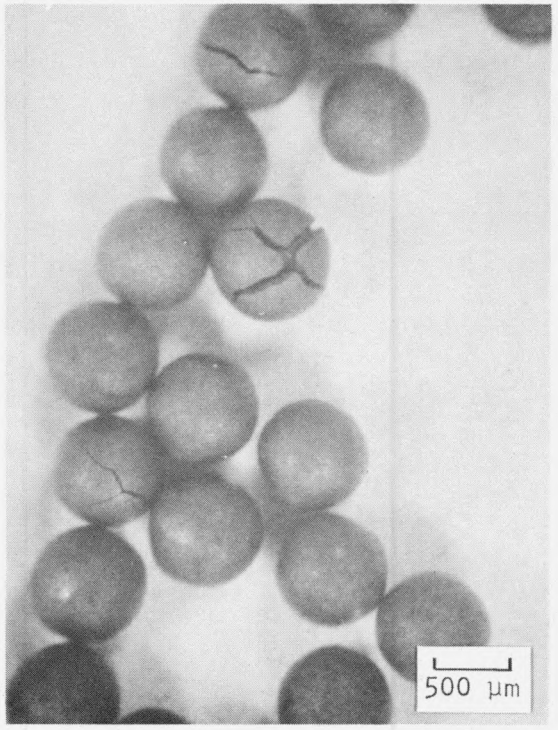


S7325-34

HT-13: 42% FAILURE
1200°C
4.4 X $10^{25}$ n/$m^2$
4.6% FIMA


S7305-50

HT-14: 98% FAILURE
1260°C
7.1 X $10^{25}$ n/$m^2$
9.1% FIMA

Fig. 5. Photomicrographs of BISO particle batch 4252-07-016 irradiated in holder 49. The increased failure with irradiation exposure was attributed to the dimensional instability of the OPyC coating which was deposited at a low coating rate of 1.4 µm/min.

early in the irradiation, the $ThO_2$ kernels had fragmented and converted to carbide, particularly in the high-temperature magazines, by the end of the irradiation.

Representative photographs of the $ThO_2$ TRISO particle batch (6252-01-023) are shown in Fig. 6. All the particle samples experienced relatively high levels of OPyC coating failure and the level of pressure vessel failure (failure of both the OPyC and SiC coatings), while zero at 20% of peak burnup, increased significantly with increasing burnup (up to 80% at full burnup).

## 4.2. METALLOGRAPHY

Five particle samples were examined metallographically to evaluate the irradiation-induced changes in the fuel particle coatings and fuel kernel microstructure. Six particles from each batch were mounted, and after grinding, the specimens were reimpregnated with mounting compound to reduce kernel pullout during polishing. The polished specimens were examined under bright-field illumination and polarized light with a Lietz metallograph.

Representative photomicrographs of batch 4252-02-015 irradiated in holder 40 of capsules HT-12, HT-13, HT-14, and HT-15 are shown in Fig. 7. Irradiation-induced changes in the $ThO_2$ fuel kernel microstructure are apparent. At a low burnup of 1.5% FIMA, small micropores were visible. After irradiation to higher burnups (≥5.8% FIMA) in capsules HT-13, HT-14, and HT-15, the kernel microstructural features were completely obliterated by the formation of larger pores and fission gas bubble agglomerations. However, the kernels remained spherical and no interactions with the surrounding buffer coating were observed, even in the HT-15 sample which was irradiated to a very high burnup of 13.8% FIMA at a maximum particle surface temperature of 1315°C which corresponds with a kernel temperature of 1365° to 1410°C.

The effects of fast neutron exposure and slight fuel kernel swelling on the pyrocarbon coatings can also be observed in Fig. 7. In the HT-12

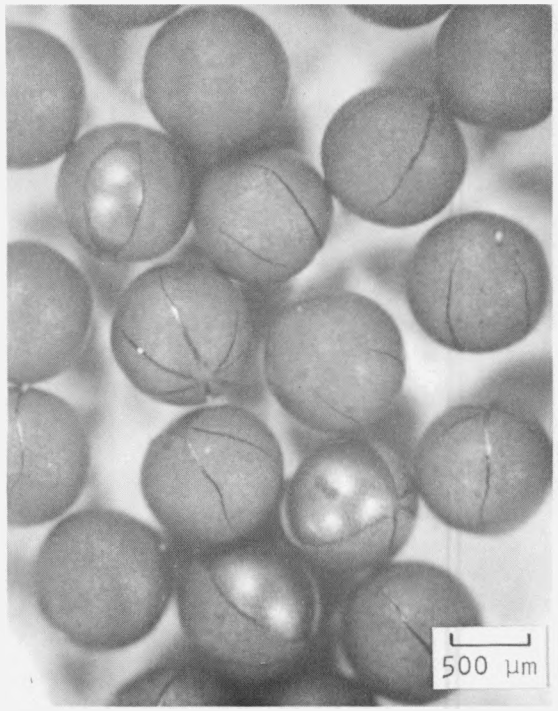


S7354-9

HT-17: 83% OPyC FAILURE
0% PV FAILURE
1070°C
2.2 X $10^{25}$ n/$m^2$
1.3% FIMA

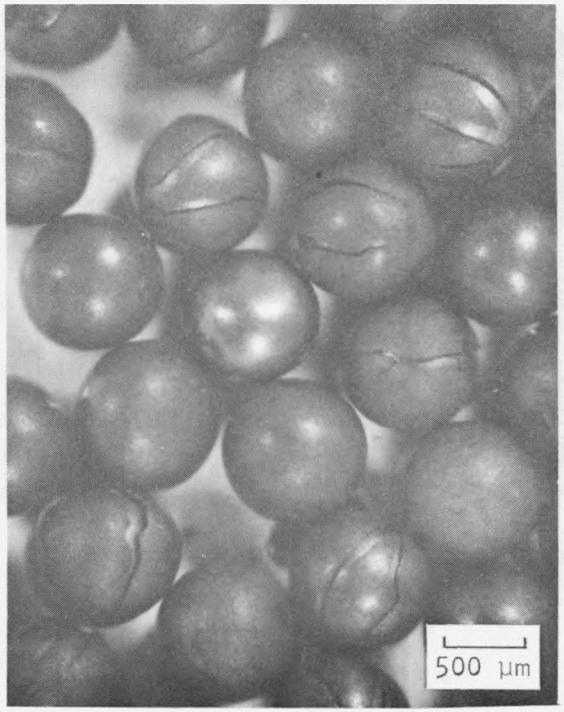


S7354-59

HT-18: 61% OPyC FAILURE
7% PV FAILURE
1130°C
4.2 X $10^{25}$ n/$m^2$
4.7% FIMA

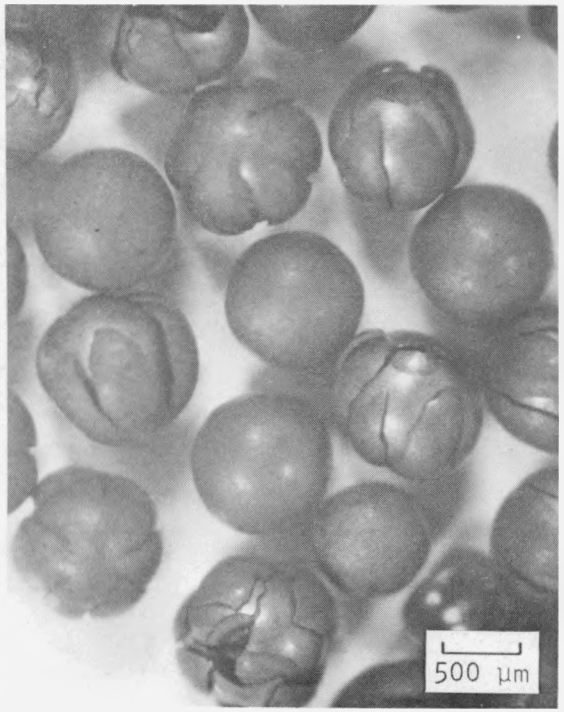


S7354-171

HT-19: 74% OPyC FAILURE
58% PV FAILURE
1160°C
6.4 X $10^{25}$ n/$m^2$
8.6% FIMA

Fig. 6. Photomicrographs of $ThO_2$ TRISO particle batch 6252-01-023 irradiated in holder 51. All samples experienced significant levels of OPyC coating failure; however, the level of pressure vessel (PV) failure increased with irradiation exposure.

sample the OPyC coating appeared nearly optically isotropic under polarized light. After irradiation to higher fast neutron exposures, a marked increase in the optical anisotropy of the OPyC coating was observed. The buffer coating densified and exhibited a marked degree of optical anisotropy in all the samples examined.

## 4.3. X-RAY RADIOGRAPHY

Samples from 38 BISO coated $ThO_2$ particle batches were radiographed to evaluate the irradiation-induced dimensional change of the fuel kernels and PyC coatings. Contact X-ray microradiographs were obtained by exposing high-resolution photographic plates to an X-ray pulse from a Picker 110 kV X-ray unit. The particle images on the radiograph plates were then examined to determine the preirradiation and postirradiation particle dimensions. These data and the calculated irradiation-induced dimensional changes are given in Table 12.

## 4.4. PARTICLE DENSITY MEASUREMENTS

Postirradiation particle density measurements were made on 32 samples of BISO $ThO_2$ particles. The samples were examined using an in-cell stereomicroscope to ensure that all the particles were intact. Each sample was then cleaned in an ultrasonic bath of 50-50 $H_2O$-$HNO_3$ for 10 min to remove any surface contamination. A density gradient column technique similar to the one described in Ref. 6 was employed to measure the density of the coated particles. Two concentrations of aqueous thallium malonate were blended to provide a uniform density gradient column medium. Without using a hot water jacket, the maximum density obtainable with this solution was 4.44 $Mg/m^3$. A density gradient curve for the liquid column was established using calibrated glass density floats. The preirradiation and postirradiation particle densities measured using a density gradient column are presented in Table 13.

For comparative purposes the postirradiation density of the particle samples was calculated from the preirradiation and postirradiation dimensions

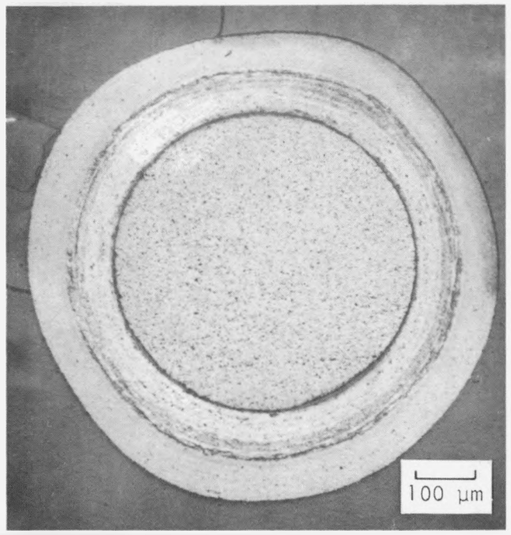


L7305-49

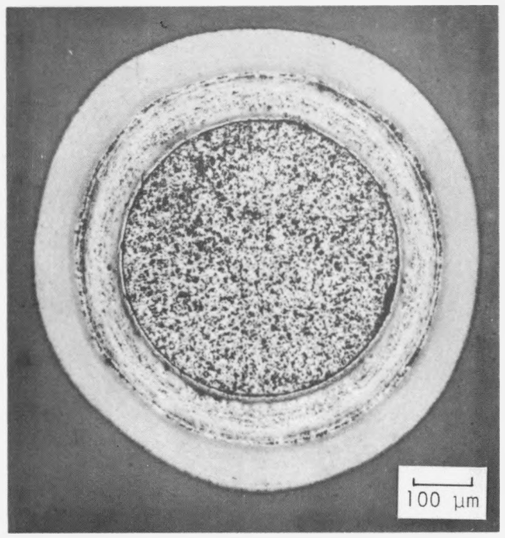


L7305-17

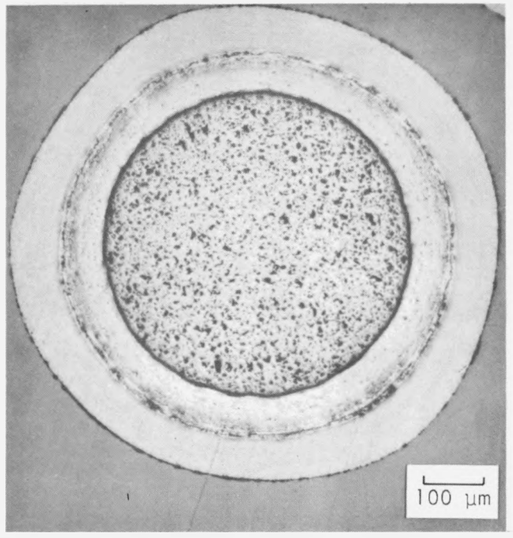


L7305-41

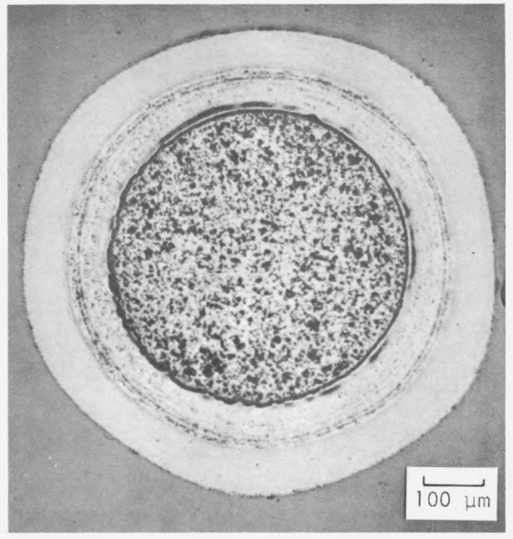


L7305-23

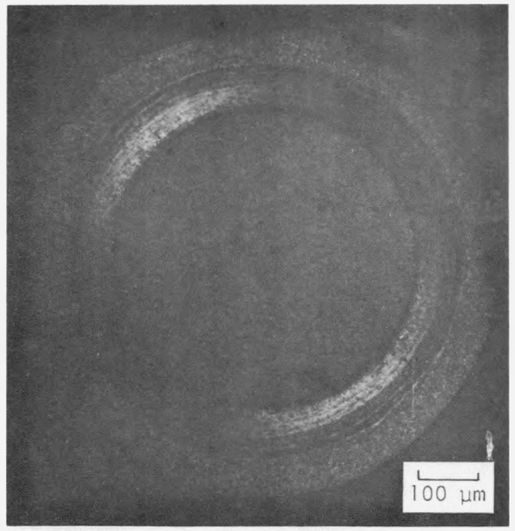


L7305-50

HT-12: 1170°C
$2.8 \times 10^{25}$ n/m$^2$
1.5% FIMA

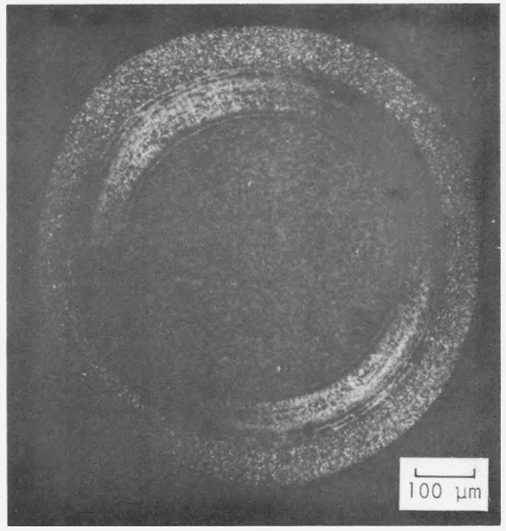


L7305-18

HT-13: 1255°C
$6.2 \times 10^{25}$ n/m$^2$
5.8% FIMA

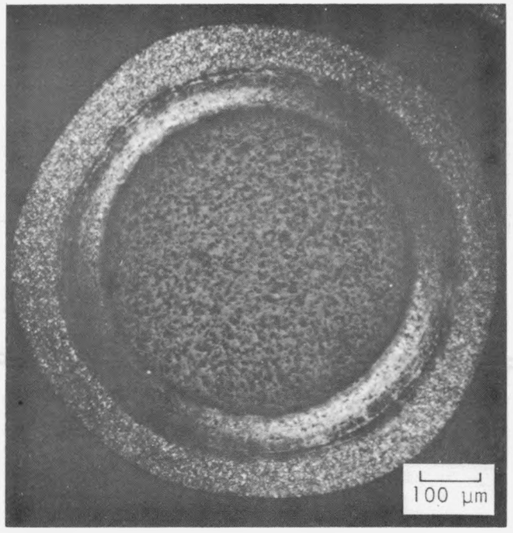


L7305-42

HT-14: 1305°C
$9.9 \times 10^{25}$ n/m$^2$
11.4% FIMA

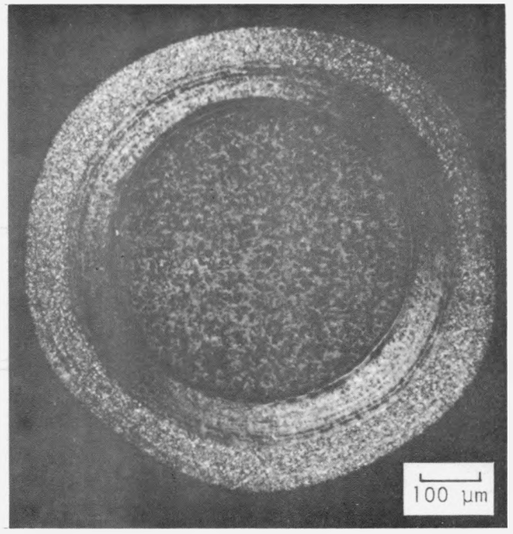


L7305-24

HT-15: 1315°C
$11.5 \times 10^{25}$ n/m$^2$
13.8% FIMA

Fig. 7. Bright-field and polarized light photomicrographs of $ThO_2$ BISO particles from batch 4252-02-015 irradiated in holder no. 40 of capsules HT-12, HT-13, HT-14, and HT-15

TABLE 12
IRRADIATION-INDUCED DIMENSIONAL CHANGES OF BISO $ThO_2$ PARTICLES

| | Irradiation Conditions | | | | Kernel Diameter | | | Coating Thickness | | | Particle Diameter | | |
|---|---|---|---|---|---|---|---|---|---|---|---|---|---|
| Batch Number | Capsule Position | Average Temp (°C) | Fast Fluence ($10^{25}$ n/m$^2$) (E > 29 fJ)$_{HTGR}$ | Burnup (% FIMA) | Preirradiation (μm) | Postirradiation (μm) | $\Delta D/D_o$ (%) | Preirradiation (μm) | Postirradiation (μm) | $\Delta T/T_o$ (%) | Preirradiation (μm) | Postirradiation (μm) | $\Delta D/D_o$ (%) |
| 4252-00-013-3 | HT-12-20 | 1325 | 3.4 | 1.8 | 404 (±16)[a] | 410 (±9) | +1.4 (±4.2) | 156 | 148 | -5.1 | 703 (±39) | 705 (±20) | +0.3 |
| -7 | HT-12-7 | 1025 | 2.2 | 1.3 | 397 (±24) | 406 (±9) | +2.3 (±6.6) | 158 | 148 | -6.3 | 703 (±37) | 701 (±19) | -0.3 |
| -8 | HT-13-7 | 1100 | 5.0 | 5.0 | 404 (±11) | 411 (±12) | +1.7 (±3.9) | 158 | 148 | -6.3 | 721 (±20) | 707 (±20) | -1.9 |
| 4252-02-015-5 | HT-12-40 | 1170 | 2.8 | 1.5 | 505 (±10) | 510 (±6) | +1.0 (±2.4) | 160 | 142 | -11.2 | 827 (±20) | 794 (±15) | -4.0 |
| -6 | HT-13-40 | 1255 | 6.2 | 5.8 | 508 (±8) | 518 (±8) | +2.0 (±2.2) | 160 | 130 | -18.8 | 828 (±19) | 789 (±15) | -4.7 |
| -7 | HT-14-40 | 1305 | 9.9 | 11.4 | 509 (±8) | 526 (±11) | +3.3 (±2.6) | 157 | 134 | -14.6 | 819 (±24) | 795 (±12) | -2.9 |
| -8 | HT-15-40 | 1315 | 11.5 | 13.8 | 509 (±8) | 524 (±8) | +2.9 (±2.2) | 161 | 132 | -18.0 | 827 (±18) | 788 (±45) | -4.7 |
| 4252-06-012-1 | HT-12-23 | 1410 | 3.5 | 1.9 | 513 (±14) | 520 (±6) | +1.4 (±3.0) | 153 | 134 | -13.1 | 818 (±19) | 787 (±10) | -3.9 |
| -5 | HT-12-10 | 1120 | 2.5 | 1.4 | 515 (±8) | 518 (±5) | +0.6 (±1.8) | 153 | 136 | -11.1 | 820 (±19) | 791 (±12) | -3.5 |
| -6 | HT-13-10 | 1230 | 5.6 | 5.5 | 516 (±7) | 518 (±9) | +0.4 (±2.2) | 156 | 127 | -18.6 | 821 (±19) | 772 (±17) | -6.0 |
| -7 | HT-14-10 | 1290 | 9.0 | 10.8 | 513 (±9) | 518 (10) | +1.2 (±3.1) | 155 | 129 | -16.8 | 822 (±14) | 776 (±16) | -5.6 |
| -8 | HT-15-10 | 1305 | 10.5 | 13.3 | 509 (±19) | 533 (±6) | +4.7 (±3.9) | 152 | 131 | -13.8 | 820 (±15) | 795 (±10) | -3.0 |
| 4252-08-014-5 | HT-12-2 | 1185 | 1.8 | 1.0 | 508 (±8) | 512 (±8) | +0.8 (±2.2) | 159 | 150 | -5.7 | 823 (±21) | 812 (±12) | -1.3 |
| 4252-07-016-5 | HT-12-49 | 1090 | 2.0 | 1.1 | 492 (±9) | 495 (±10) | +0.6 (±2.6) | 96 | 85 | -11.5 | 680 (±15) | 665 (±12) | -2.2 |
| -6 | HT-13-49 | 1200 | 4.4 | 4.6 | 492 (±8) | 498 (±10) | +1.2 (±2.6) | 96 | 86 | -10.4 | 683 (±12) | 669 (±14) | -2.0 |
| 6542-01-013-7 | HT-17-40 | 1170 | 3.3 | 2.0 | 509 (±3) | 511 (±3) | +0.4 (±0.8) | 166 | 144 | -13.3 | 842 (±14) | 798 (±11) | -5.2 |
| -8 | HT-18-40 | 1250 | 6.8 | 6.6 | 509 (±8) | 517 (±4) | +1.6 (±1.8) | 166 | 138 | -16.9 | 840 (±16) | 794 (±12) | -5.5 |
| -9 | HT-19-40 | 1290 | 10.1 | 11.7 | 511 (±3) | 523 (±6) | +2.3 (±1.3) | 168 | 142 | -15.5 | 846 (±12) | 807 (±18) | -4.6 |
| -10 | HT-17-27 | 1435 | 4.2 | 2.4 | 512 (±3) | 515 (±3) | +0.6 (±0.8) | 166 | 142 | -14.5 | 845 (±17) | 798 (±13) | -5.4 |
| -11 | HT-18-27 | 1500 | 8.6 | 7.9 | 511 (±3) | 518 (±4) | +1.4 (±1.0) | 168 | 143 | -14.9 | 848 (±14) | 804 (±10) | -5.2 |
| 6542-01-023-1 | HT-17-42 | 1140 | 3.2 | 1.9 | 490 (±10) | 491 (±11) | +0.2 (±3.0) | 152 | 132 | -13.2 | 793 (±19) | 756 (±21) | -4.7 |
| -2 | HT-18-42 | 1245 | 6.4 | 6.5 | 486 (±10) | 511 (±18) | +5.1 (±4.2) | 151 | 122 | -19.2 | 788 (±21) | 754 (±21) | -4.3 |
| -4 | HT-17-29 | 1415 | 4.2 | 2.4 | 483 (±11) | 493 (±9) | +2.1 (±2.9) | 138 | 132 | -4.3 | 759 (±41) | 756 (±16) | -0.4 |
| -5 | HT-18-29 | 1505 | 8.5 | 7.8 | 479 (±17) | 512 (±12) | +6.9 (±4.4) | 150 | 124 | -17.3 | 779 (±28) | 761 (±15) | -2.3 |
| 6542-02-023-1 | HT-17-43 | 1115 | 3.1 | 1.9 | 475 (±14) | 478 (±11) | +0.6 (±3.6) | 154 | 144 | -6.5 | 784 (±26) | 767 (±19) | -2.2 |
| -2 | HT-18-43 | 1215 | 6.1 | 6.3 | 476 (±13) | 486 (±12) | +2.1 (±3.7) | 154 | 136 | -11.7 | 783 (±24) | 756 (±19) | -3.3 |
| -3 | HT-19-43 | 1260 | 9.3 | 11.2 | 472 (±12) | 485 (±14) | +2.8 (±4.0) | 156 | 138 | -11.5 | 783 (±28) | 760 (±22) | -2.9 |
| -4 | HT-17-30 | 1395 | 4.2 | 2.4 | 477 (±16) | 479 (±16) | +0.4 (±4.5) | 155 | 140 | -9.7 | 787 (±28) | 758 (±27) | -3.7 |
| -5 | HT-18-30 | 1485 | 8.5 | 7.7 | 474 (±14) | 480 (±16) | +1.3 (±4.6) | 154 | 140 | -9.1 | 781 (±31) | 759 (±25) | -2.8 |
| -6 | HT-19-30 | 1520 | 12.6 | 13.4 | 474 (±13) | 487 (±16) | +2.7 (±4.3) | 156 | 154 | -1.3 | 786 (±27) | 794 (±31) | +1.0 |
| 6542-02-033-1 | HT-17-45 | 1100 | 2.9 | 1.7 | 471 (±12) | 474 (±10) | +0.6 (±3.1) | 146 | 134 | -8.2 | 763 (±22) | 742 (±19) | -2.8 |
| -4 | HT-17-32 | 1395 | 4.1 | 2.4 | 471 (±13) | 475 (±10) | +0.8 (±3.3) | 151 | 130 | -13.9 | 773 (±23) | 736 (±15) | -4.8 |
| 6542-16-013-1 | HT-17-46 | 1170 | 2.9 | 1.6 | 484 (±13) | 490 (±5) | +1.2 (±2.8) | 96 | 87 | -9.4 | 676 (±23) | 664 (±20) | -1.8 |
| -2 | HT-18-46 | 1280 | 5.5 | 5.7 | 489 (±13) | 502 (±11) | +2.7 (±3.5) | 98 | 83 | -15.3 | 686 (±17) | 668 (±11) | -3.4 |
| -4 | HT-17-33 | 1445 | 4.1 | 2.4 | 488 (±14) | 496 (±8) | +1.6 (±3.2) | 84 | 84 | 0 | 656 (±40) | 664 (±9) | +1.2 |
| 6542-17-013-1 | HT-17-48 | 1105 | 2.5 | 1.5 | 497 (±9) | 496 (±7) | -0.2 (±2.3) | 161 | 144 | -10.6 | 819 (±21) | 784 (±14) | -4.3 |
| -2 | HT-18-48 | 1195 | 5.1 | 5.4 | 497 (±8) | 502 (±6) | +1.0 (±2.0) | 158 | 144 | -8.9 | 814 (±22) | 790 (±13) | -2.8 |
| -4 | HT-17-35 | 1390 | 4.0 | 2.3 | 501 (±9) | 501 (±8) | 0 | 159 | 144 | -9.4 | 819 (±21) | 790 (±16) | -3.5 |

[a] Numbers in parentheses are standard deviations.

TABLE 13
IRRADIATION-INDUCED Ddensification OF BISO $ThO_2$ PARTICLES

| Batch Number | Irradiation Conditions | | | | Particle Density ($Mg/m^3$) | | | Irradiation-Induced Densification (%) | |
|---|---|---|---|---|---|---|---|---|---|
| | | | | | Gradient Column | | X-ray Radiography | | |
| | Capsule Position | Average Temp (°C) | Fast Fluence ($10^{25}$ $n/m^2$) (E > 29 fJ)$_{HTGR}$ | Burnup (% FIMA) | Preirradiation | Postirradiation | Postirradiation[a] | Column | X-ray Radiography |
| 4252-00-013-3 | HT-12-20 | 1325 | 3.4 | 1.8 | 3.30 (±0.044)[b] | 3.50 (±0.030) | 3.27 (±0.62) | +6.1 (±1.6) | -0.8 |
| -7 | HT-12-7 | 1025 | 2.2 | 1.3 | 3.30 (±0.044) | 3.51 (±0.027) | 3.33 (±0.61) | +6.4 (±1.6) | +0.9 |
| -8 | HT-13-7 | 1100 | 5.0 | 5.0 | 3.30 (±0.044) | 3.77 (±0.099) | 3.50 (±0.40) | +14.2 (±3.3) | +6.1 |
| 4252-02-015-5 | HT-12-40 | 1170 | 2.8 | 1.5 | 3.58 (±0.021) | 4.07 (±0.024) | 4.05 (±0.34) | +13.7 (±0.9) | +13.0 |
| -6 | HT-13-40 | 1255 | 6.2 | 5.8 | 3.58 (±0.021) | 4.20 (±0.039) | 4.14 (±0.34) | +17.3 (±1.2) | +15.6 |
| -7 | HT-14-40 | 1305 | 9.9 | 11.4 | 3.58 (±0.021) | 4.03 (±0.018) | 3.91 (±0.37) | +12.6 (±0.8) | +9.3 |
| -8 | HT-15-40 | 1315 | 11.5 | 13.8 | 3.58 (±0.021) | 4.02 (±0.018) | 4.14 (±0.69) | +12.3 (±0.8) | +15.6 |
| 4252-06-012-1 | HT-12-23 | 1410 | 3.5 | 1.9 | 3.81 (±0.015) | 4.25 (±0.071) | 4.28 (±0.31) | +11.5 (±1.9) | +13.3 |
| -5 | HT-12-10 | 1120 | 2.5 | 1.4 | 3.81 (±0.015) | 4.16 (±0.064) | 4.24 (±0.33) | +9.2 (±1.7) | +11.4 |
| -6 | HT-13-10 | 1230 | 5.6 | 5.5 | 3.81 (±0.015) | 4.01 (±0.087) | 4.58 (±0.39) | +5.2 (±2.3) | +20.3 |
| -7 | HT-14-10 | 1290 | 9.0 | 10.8 | 3.81 (±0.015) | 4.04 (±0.018) | 4.53 (±0.33) | +6.0 (±0.6) | +18.9 |
| -8 | HT-15-10 | 1305 | 10.5 | 13.3 | 3.81 (±0.015) | 4.19 (±0.017) | 4.18 (±0.26) | +10.0 (±0.6) | +9.7 |
| 4252-08-014-5 | HT-12-2 | 1185 | 1.8 | 1.0 | 3.84 (±0.010) | 4.11 (±0.067) | 4.00 (±0.34) | +7.0 (±1.8) | +4.1 |
| 4252-07-016-5 | HT-12-49 | 1090 | 2.0 | 1.1 | 4.84[c] (±0.031) | (d) | 5.17 (±0.42) | -- | +6.8 |
| -6 | HT-13-49 | 1200 | 4.4 | 4.6 | 4.84[c] (±0.031) | (d) | 5.15 (±0.41) | -- | +6.4 |
| 6542-01-013-7 | HT-17-40 | 1170 | 3.3 | 2.0 | 3.44 (±0.031) | 4.10 (±0.089) | 4.04 (±0.24) | +19.2 (±2.7) | +17.5 |
| -8 | HT-18-40 | 1250 | 6.8 | 6.6 | 3.44 (±0.031) | 4.10 (±0.073) | 4.07 (±0.27) | +19.2 (±2.3) | +18.4 |
| -9 | HT-19-40 | 1290 | 10.1 | 11.7 | 3.44 (±0.031) | 3.85 (±0.068) | 3.96 (±0.29) | +11.9 (±2.2) | +15.2 |
| -10 | HT-17-27 | 1435 | 4.2 | 2.4 | 3.44 (±0.031) | 3.92 (±0.264) | 4.07 (±0.27) | +14.0 (±7.8) | +18.3 |
| -11 | HT-18-27 | 1500 | 8.6 | 7.9 | 3.44 (±0.031) | 3.91 (±0.056) | 4.04 (±0.23) | +13.7 (±1.9) | +17.3 |
| 6542-01-023-1 | HT-17-42 | 1140 | 3.2 | 1.9 | 3.54 (±0.013) | 4.28 (±0.030) | 4.09 (±0.41) | +20.9 (±0.9) | +15.4 |
| -2 | HT-18-42 | 1245 | 6.4 | 6.5 | 3.54 (±0.013) | 4.42 (±0.003) | 4.04 (±0.43) | +24.9 (±0.4) | +14.1 |
| -4 | HT-17-29 | 1415 | 4.2 | 2.4 | 3.54 (±0.013) | 4.25 (±0.020) | 3.58 (±0.62) | +20.1 (±0.7) | +1.2 |
| -5 | HT-18-29 | 1505 | 8.5 | 7.8 | 3.54 (±0.013) | 3.97 (±0.060) | 3.80 (±0.45) | +12.1 (±1.7) | +7.3 |
| 6542-02-023-1 | HT-17-43 | 1115 | 3.1 | 1.9 | 3.45 (±0.019) | 3.79 (±0.020) | 3.68 (±0.44) | +9.9 (±0.8) | +6.8 |
| -2 | HT-18-43 | 1215 | 6.1 | 6.3 | 3.45 (±0.019) | 4.07 (±0.052) | 3.82 (±0.42) | +18.0 (±1.6) | +10.7 |
| -3 | HT-19-43 | 1260 | 9.3 | 11.2 | 3.45 (±0.019) | 4.01 (±0.102) | 3.77 (±0.49) | +16.2 (±3.0) | +9.4 |
| -4 | HT-17-30 | 1170 | 3.3 | 2.0 | 3.45 (±0.019) | 3.92 (±0.100 | 3.86 (±0.54) | +13.6 (±3.0) | +11.9 |
| -5 | HT-18-30 | 1485 | 8.5 | 7.7 | 3.45 (±0.019) | 3.83 (±0.134) | 3.76 (±0.55) | +11.0 (±3.9) | +9.0 |
| -6 | HT-19-30 | 1520 | 12.6 | 13.4 | 3.45 (±0.019) | 3.25 (±0.325) | 3.35 (±0.53) | -5.8 (±9.4) | -2.9 |
| 6542-02-033-1 | HT-17-45 | 1100 | 2.9 | 1.7 | 3.54 (±0.001) | 4.13 (±0.017) | 3.85 (±0.42) | +16.7 (±0.5) | +8.7 |
| -4 | HT-17-32 | 1395 | 4.1 | 2.4 | 3.54 (±0.001) | 4.16 (±0.043) | 4.10 (±0.40) | +17.5 (±1.2) | +15.9 |
| 6542-16-013-1 | HT-17-46 | 1170 | 2.9 | 1.6 | 4.78[c] (±0.021) | (d) | 5.04 (±0.66) | -- | +5.4 |
| -2 | HT-18-46 | 1280 | 5.5 | 5.7 | 4.78[c] (±0.021) | (d) | 5.18 (±0.44) | -- | +8.3 |
| -4 | HT-17-33 | 1445 | 4.1 | 2.4 | 4.78[c] (±0.021) | (d) | 4.61 (±0.88) | -- | -3.6 |
| 6542-17-013-1 | HT-17-48 | 1105 | 2.5 | 1.5 | 3.58 (±0.030) | (d) | 4.08 (±0.35) | -- | +14.0 |
| -2 | HT-18-48 | 1195 | 5.1 | 5.4 | 3.58 (±0.030) | 3.95 (±0.042) | 3.90 (±0.35) | +10.3 (±1.4) | +9.0 |
| -4 | HT-17-35 | 1390 | 4.0 | 2.3 | 3.58 (±0.030) | 4.08 (±0.028) | 3.99 (±0.36) | +14.0 (±1.1) | +11.4 |

[a] Calculated from preirradiation density and irradiation-induced volume change using Eq. 2.

[b] Numbers in parentheses are standard deviations.

[c] Density measured using a gradient column with a hot water jacket.

[d] Particle densities >4.44 $Mg/m^3$ could not be measured because a gradient column with a hot water jacket could not be set up in the hot cell.

determined by X-ray radiography. By assuming the mass of the particles remained constant during irradiation, the postirradiation particle density was calculated using the following equation:

$$\rho = \rho_o \left(\frac{D_o}{D_f}\right)^3 , \qquad (2)$$

where $\rho$ = postirradiation particle density,
$\rho_o$ = preirradiation particle density,
$D_o$ = preirradiation particle diameter,
$D_f$ = postirradiation particle diameter.

The postirradiation particle densities calculated using Eq. 2 are given in Table 13.

# 5. DISCUSSION

## 5.1. FERTILE PARTICLE IRRADIATION PERFORMANCE

### 5.1.1. BISO $ThO_2$ Particles

The primary objective of this series of HT experiments was to evaluate the irradiation performance of BISO coated $ThO_2$ particles as a function of several coating parameters which included thickness, density, coating rate, and anisotropy. The results revealed a stronger correlation between OPyC coating rate or anisotropy and particle survival than with the other parameters tested. Samples from BISO particle batches 4252-02-015 and 4252-06-012 exhibited the best irradiation performance of the batches tested in capsules HT-12 through HT-15. These particle batches had OPyC coatings which were applied at mean rates of 3.7 to 5.8 μm/min. No particle failure was observed in batch 4252-02-015 irradiated in the low-temperature magazines to fast neutron exposures up to $9.9 \times 10^{25}$ $n/m^2$ $(E > 29\ fJ)_{HTGR}$ and heavy metal burnups up to 11.4% FIMA. With the exception of one particle in HT-12, no particle failure was observed in batch 4252-06-012 irradiated in the low-temperature magazines to fast neutron exposures up to $10.5 \times 10^{25}$ $n/m^2$ $(E > 29\ fJ)_{HTGR}$ and heavy metal burnups up to 13.3% FIMA. In contrast, particle failure levels in batch 4252-01-071, which had a relatively low mean OPyC coating rate of 1.6 μm/min reached 34% and 100% during irradiation in the low-temperature magazines to fast neutron exposures of 5.0 and $8.1 \times 10^{25}$ $n/m^2$ $(E > 29\ fJ)_{HTGR}$, respectively.

In the HT-17 through HT-19 series, BISO $ThO_2$ particle batches (6542-01-013 and 6542-02-023 having OPyC coatings deposited at mean rates of 10.6 and 8.2 μm/min exhibited the best performance. Particle batches having a

similar coating design but with OPyC coatings deposited at a mean rate ≤2.7 μm/min exhibited significantly higher levels of particle failure.

The levels of OPyC coating failure observed in the BISO $ThO_2$ particle samples have been plotted as a function of mean OPyC coating rate in Fig. 8. Particle batches having a nonconservative coating design, i.e., buffer coating thicknesses <48 μm, have not been included. The strong correlation between OPyC coating performance and coating rate is apparent. After irradiation in the low-temperature magazines to fast neutron fluences ranging from 6.0 to 10.0 x $10^{25}$ $n/m^2$, particle batches with mean coating rates <2.7 μm/min exhibited high levels of OPyC coating failure. Particle batches with mean coating rates >3.8 μm/min did not experience any OPyC coating failure, with the exception of batch 6542-02-023. The performance of this batch was anomolous in that the particle samples tested in the high-temperature magazines consistently exhibited better performance than those tested in the low-temperature magazines.

The correlation between particle performance and OPyC coating rate is related to the higher degree of preferred orientation of PyC crystallite produced at low coating rates. The anisotropy of PyC coatings increases significantly as the deposition rate falls below ∿3.0 μm/min (Ref. 7). Anisotropic PyC coatings are more dimensionally unstable and hence exhibit higher failure levels than more isotropic coatings during irradiation to high fast neutron exposures (Refs. 8-10). The OPyC anisotropy of the HT samples was evaluated prior to irradiation using an optical technique which measured the anisotropy in terms of a relative OPTAF unit. These data, shown in Table 1, are somewhat scattered but show the trend of high optical anisotropy with decreasing OPyC coating rate. A more accurate technique to evaluate PyC anisotropy is under development at GA and will be used in future studies.

Relative high failure rates were observed in four batches (4252-00-013, 4252-03-012, 4252-07-016, and 4252-08-014) tested in capsules HT-12 through HT-15. These batches had anisotropic OPyC coatings deposited at relative low coating rates (0.6 to 2.4 μm/min). However, the poor irradiation

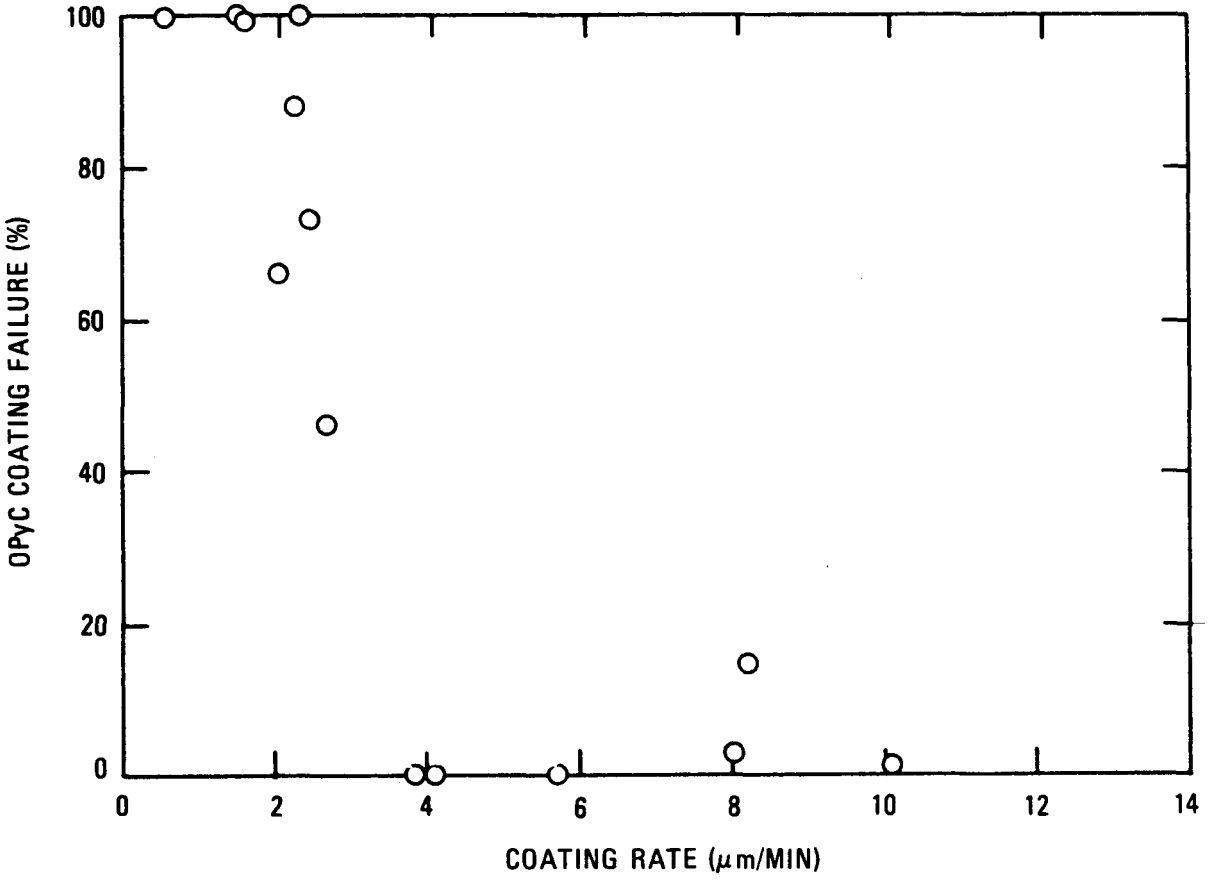


Fig. 8. OPyC coating failure versus coating rate for BISO $ThO_2$ particles irradiated in the low-temperature HT magazines (1145° to 1305°C) to fast neutron fluences ranging from 6.0 to 10.0 x $10^{25}$ $n/m^2$ $(E > 29\ fJ)_{HTGR}$

performance of the anisotropic coatings was accentuated by the presence of a large radial gradient in anisotropy across the coatings. Under polarized light the optical anisotropic gradient in these coatings is visible, as shown in Figs. A-1, A-4, A-6, and A-7. The OPyC coatings of the three remaining batches tested in the HT-12 through HT-15 series were relatively free of any gradient in anisotropy. Particle samples from the parent batch of 4252-00-013 were also irradiated in capsule P13N. The relative optical anisotropy across the OPyC coating was measured for eight particles from this batch using an apparatus developed by ÖSGAE of Seibersdorf, Austria (Ref. 11). The data are plotted in Fig. 9 in terms of the optical Bacon anisotropy factor $(BAF)_o$ versus radial position across the coating. The inner 30-μm region of the OPyC coating is highly anisotropic near the outer surface. The capsule P13N results (Ref. 12) revealed that these coatings were unstable during irradiation to a fast neutron fluence beyond $\sim 4.5 \times 10^{25}$ n/m$^2$ $(E > 29\ fJ)_{HTGR}$. At higher irradiation exposures cracks formed in the highly anisotropic inner region of the OPyC coating and propagated through the coating causing it to fail. This type of coating defect is due to a transient temperature drop in the coater during the initial application of the OPyC coating. These severe anisotropy gradients have been eliminated in subsequent BISO coated particle batches by proper control of the coating operation.

The effect of OPyC density on BISO coating irradiation performance could not be quantitatively evaluated from the samples tested. The high-density (1.96 to 2.02 Mg/m$^3$) OPyC coatings were all applied at low coating rates. Failure of these samples was attributed to the dimensional instability of the anisotropic coatings rather than the high density. However, three batches with OPyC coatings deposited at high rates were tested. Batches 6542-01-013 and 4252-06-012 had an OPyC coating density of 1.82 Mg/m$^3$ and batch 6542-02-023 had an OPyC coating density of 1.94 Mg/m$^3$. The performance of these samples in the low-temperature magazines was similar. However, in the high-temperature magazines the batch with the higher OPyC density of 1.94 Mg/m$^3$ exhibited better performance than the two batches having OPyC coating densities of 1.82 Mg/m$^3$. These results are consistent

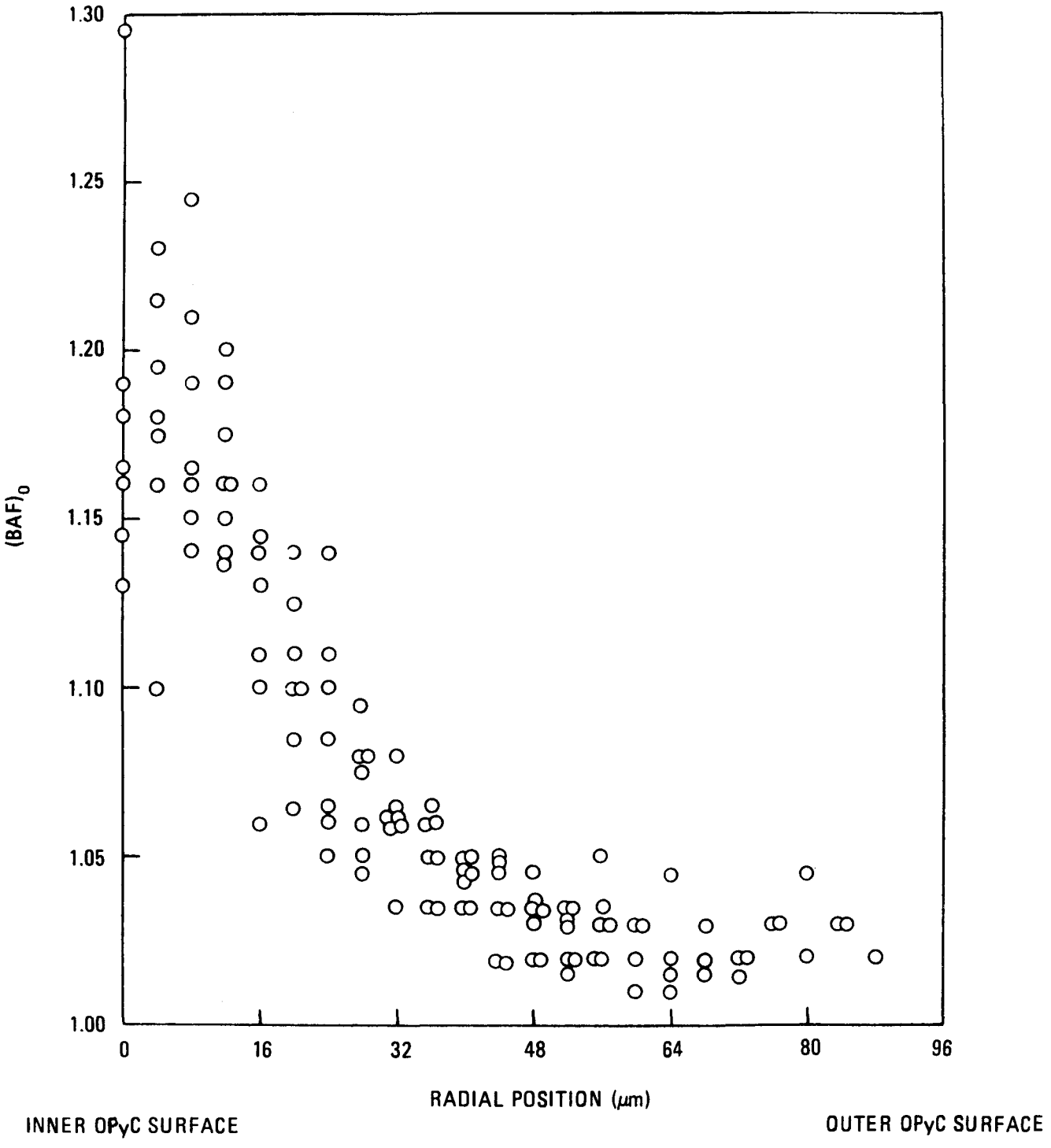


Fig. 9. Optical Bacon anisotropy factor $(BAF)_0$ versus radial position in OPyC coating in BISO particle batch 4252-00-013 used in P13N

with data obtained from capsules P13R and P13S, which indicate that OPyC coatings with densities $\geq$1.85 Mg/m$^3$ are necessary to ensure BISO particle survival at temperatures above $\sim$1250°C as long as the anisotropy of the OPyC coating is low (Ref. 13).

The poor irradiation performance of OPyC coatings deposited at low rates precluded a meaningful evaluation of the coating designs tested. However, it was apparent that the coating design of the four batches (4252-07-016, 4252-08-014, 6542-16-013 and 6542-17-013) tested with buffer coating thicknesses ranging from 44 to 48 μm was nonconservative. These samples exhibited failure at lower fluences and burnups than all the other batches, independent of the OPyC coating thicknesses.

### 5.1.2. TRISO $ThO_2$ Particles

One batch of TRISO coated $ThO_2$ particles was tested in the HT-17 through HT-19 series to provide guidance for further design improvements. This was the first full burnup irradiation test of TRISO $ThO_2$ particles.

All the TRISO $ThO_2$ particle samples exhibited high failure levels as indicated in Table 11. The OPyC coating failure levels were higher than the SiC coating failure fractions. This indicates that failure of the OPyC coating evidently preceded the loss of integrity of the SiC coating, which probably failed by a pressure vessel mechanism. Recent data on large-diameter TRISO particles have indicated that failure of the OPyC coating can have a significant effect on the SiC coating integrity during irradiation to full burnup. The TRISO particle OPyC coatings were applied at a batch mean coating rate of 3.0 μm/min. These data are consistent with other results (Refs. 13, 14) which indicate that a batch mean OPyC coating rate of 3.0 μm/min on large-diameter TRISO particles results in sufficiently high OPyC coating anisotropy that integrity of the OPyC coating cannot be ensured during irradiation to high fast neutron exposures.

The levels of pressure vessel failure (failure of both the OPyC and SiC coatings) observed in the TRISO $ThO_2$ samples are plotted in Fig. 10 as a function of burnup. The level of pressure vessel failure increased with increasing burnup and was higher in the high-temperature magazines, as would be expected. Since the samples were split from one parent batch, much of the scatter probably resulted from the small sample size and from being unable to adequately characterize levels of pressure vessel failure in TRISO particles by visual examination alone.

The high levels of pressure vessel failure observed in the TRISO $ThO_2$ particle samples at burnups <7.5% (LHTGR peak fertile burnup) indicate this particle design is nonconservative. However, these data provide a good basis for performance model studies and an improved particle design.

## 5.2. IRRADIATION-INDUCED PARTICLE DIMENSIONAL CHANGE

### 5.2.1. BISO Particles

During irradiation BISO coated particles undergo a dimensional change resulting from fast-neutron-induced dimensional changes in the OPyC coating and expansion due to the buildup of internal fission gas pressure. The mechanical behavior of BISO particles during irradiation is complex and must be interpreted using an analytical stress model. Such a BISO particle stress model has been developed at GA and will be used to predict BISO particle irradiation-induced dimensional changes and coating performance (Ref. 15). Empirical dimensional change data are required for verification of the model. The dimensional change can be determined experimentally by radiography (measurement of the change in particle diameter) or by measuring the total particle density before and after irradiation. These measurements were made on eleven batches of BISO $ThO_2$ particles irradiated in this series of HT experiments. The data are reported in Tables 12 and 13. These data were used in the initial comparison of the BISO coating stress model with experimental results (Ref. 16).

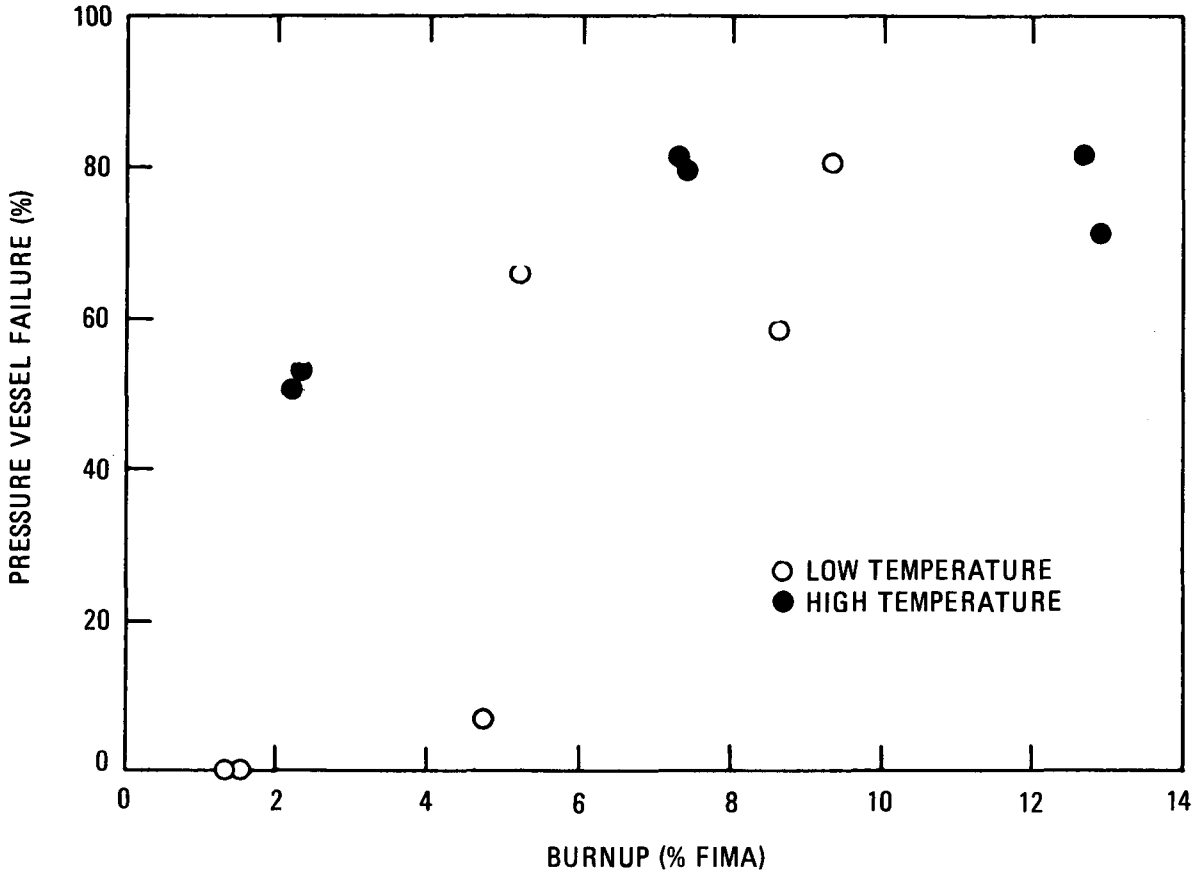


Fig. 10. Pressure vessel failure versus burnup for $ThO_2$ TRISO particles irradiated in HT-17 through HT-19

Irradiation-induced BISO particle diametral changes ranged from +1.2 to -6.0%. The particles shrank early during irradiation due to the irradiation-induced shrinkage of the OPyC coating. After irradiation to higher exposures some particles started to expand. This volumetric expansion was due to a turnaround in the densification of the OPyC coating and/or the stress generated by the buildup of internal fission gas pressure.

The total particle densities determined for three batches (4252-02-015, 6542-01-013, and 6542-02-023) by density gradient column measurements and radiography are plotted as a function of fast neutron fluence in Figs. 11, 12, and 13, respectively. The particle densities determined by the two techniques are in good agreement for these three batches. The standard deviation in the particle densities determined by radiography are not shown in Figs. 11 through 13 but are given in Table 13. In some of the remaining batches agreement between the two techniques is good with the exception of one or two samples. These differences could be due to random experimental error. In batches 4252-00-013 and 6542-01-023 the particle densities determined by radiography were consistently less than the densities measured using the gradient column. The source of this systematic error was not identified; however, it could result from an erroneous measurement of the preirradiation particle density or diameter. It could also be associated with impregnation of the density column fluid into the OPyC coating.

### 5.2.2. $ThO_2$ Fuel Kernel Swelling

The diameter of the $ThO_2$ fuel kernels was measured before and after irradiation (Table 12). From these data a measure of the irradiation-induced diametral swelling in $ThO_2$ kernels was obtained. The results are plotted in Fig. 14. The kernel swelling increased with increasing burnup, as would be expected, and ranged from -0.2 to +6.9%. No temperature dependence on kernel swelling was observed; however, this may have been masked by the relative large uncertainty in the measured values shown in

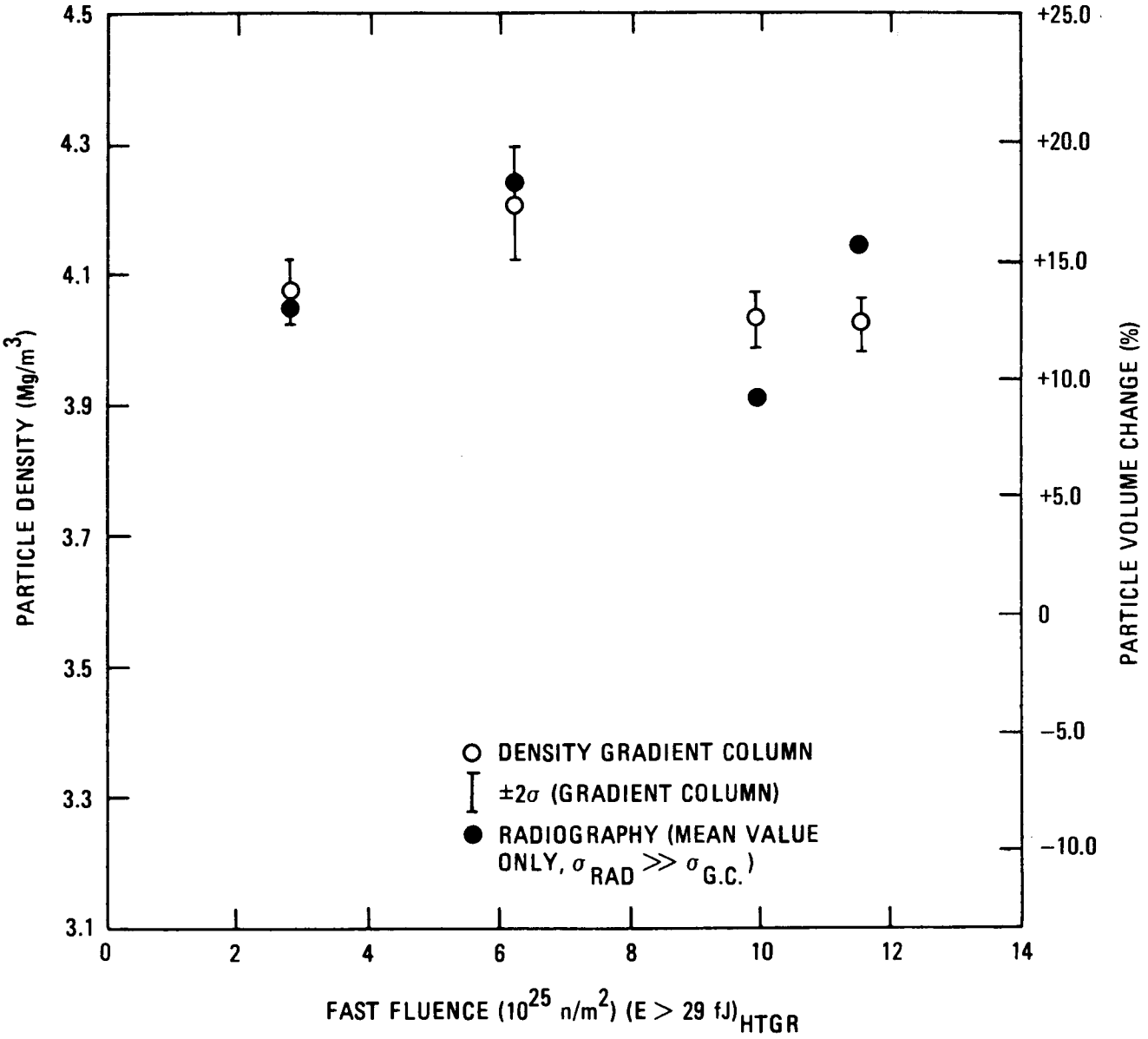


Fig. 11. Density and volume changes versus fast neutron fluence of BISO $ThO_2$ particles (4252-02-015) irradiated at 1170° to 1315°C in capsules HT-12 through HT-15

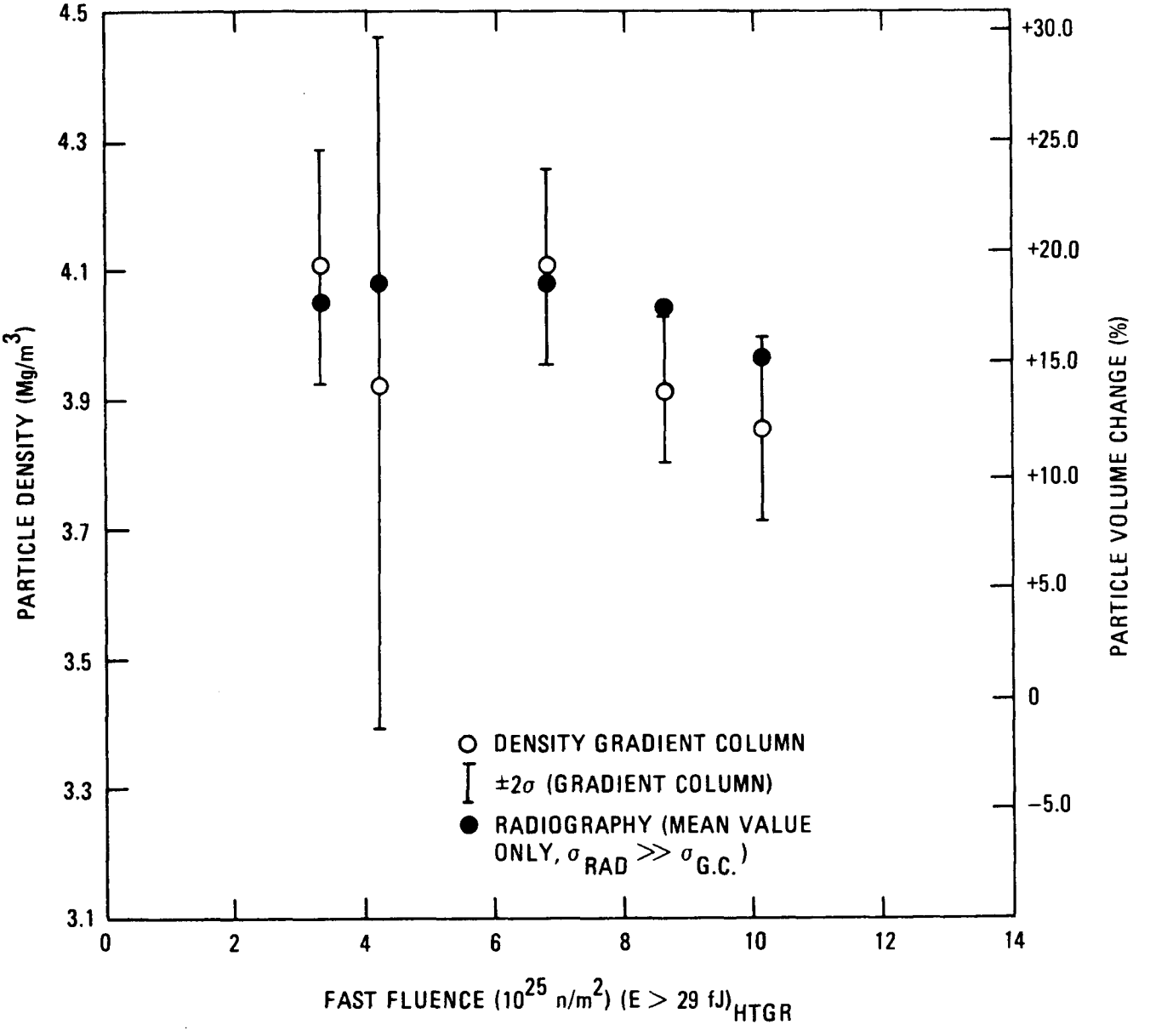


Fig. 12. Density and volume changes versus fast neutron fluence of BISO $ThO_2$ particles (6542-01-013) irradiated at 1170° to 1500°C in capsules HT-17 through HT-19

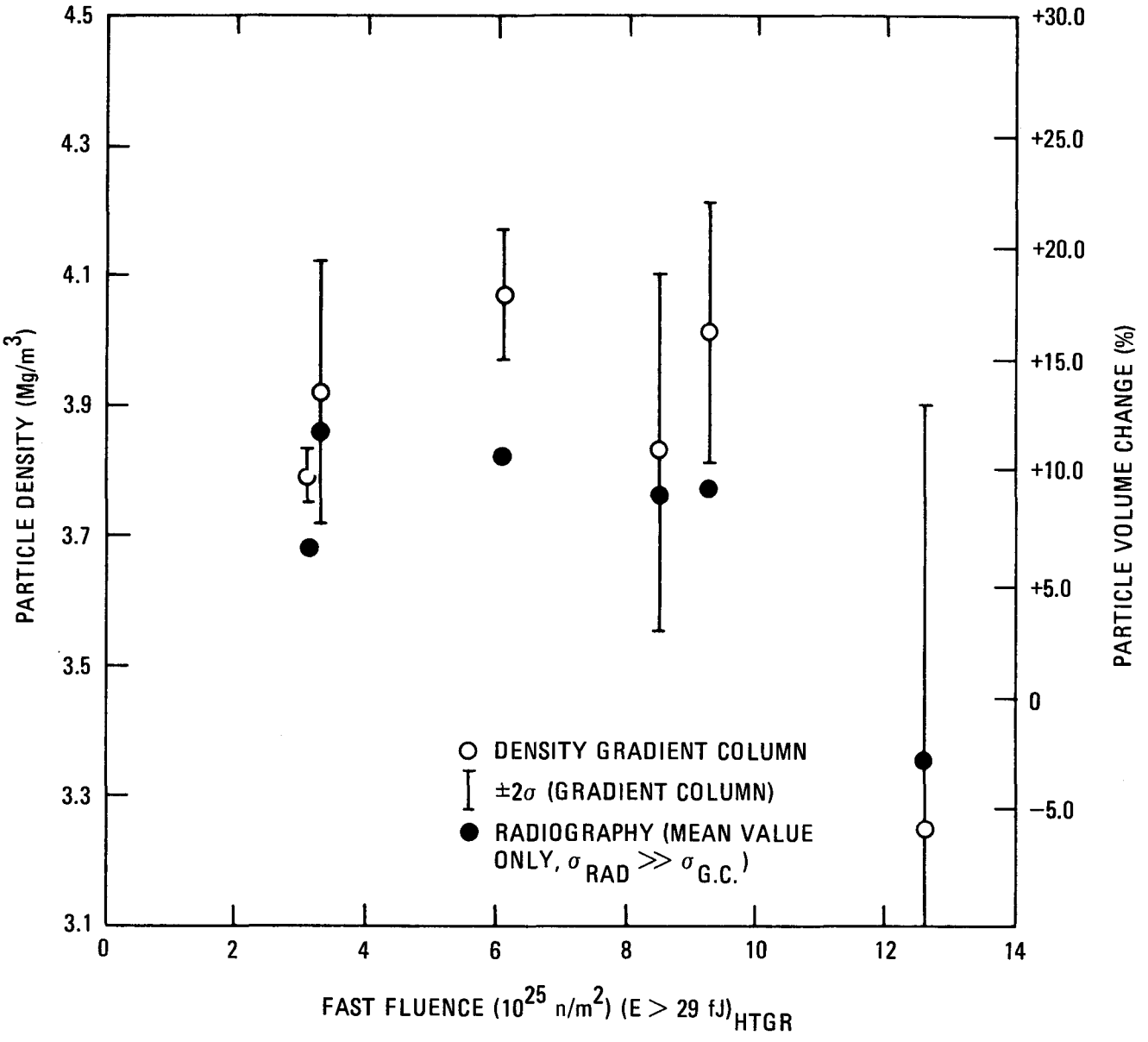


Fig. 13. Density and volume changes versus fast neutron fluence of BISO $ThO_2$ particles (6542-02-023) irradiated at 1115° to 1520°C in capsules HT-17 through HT-19

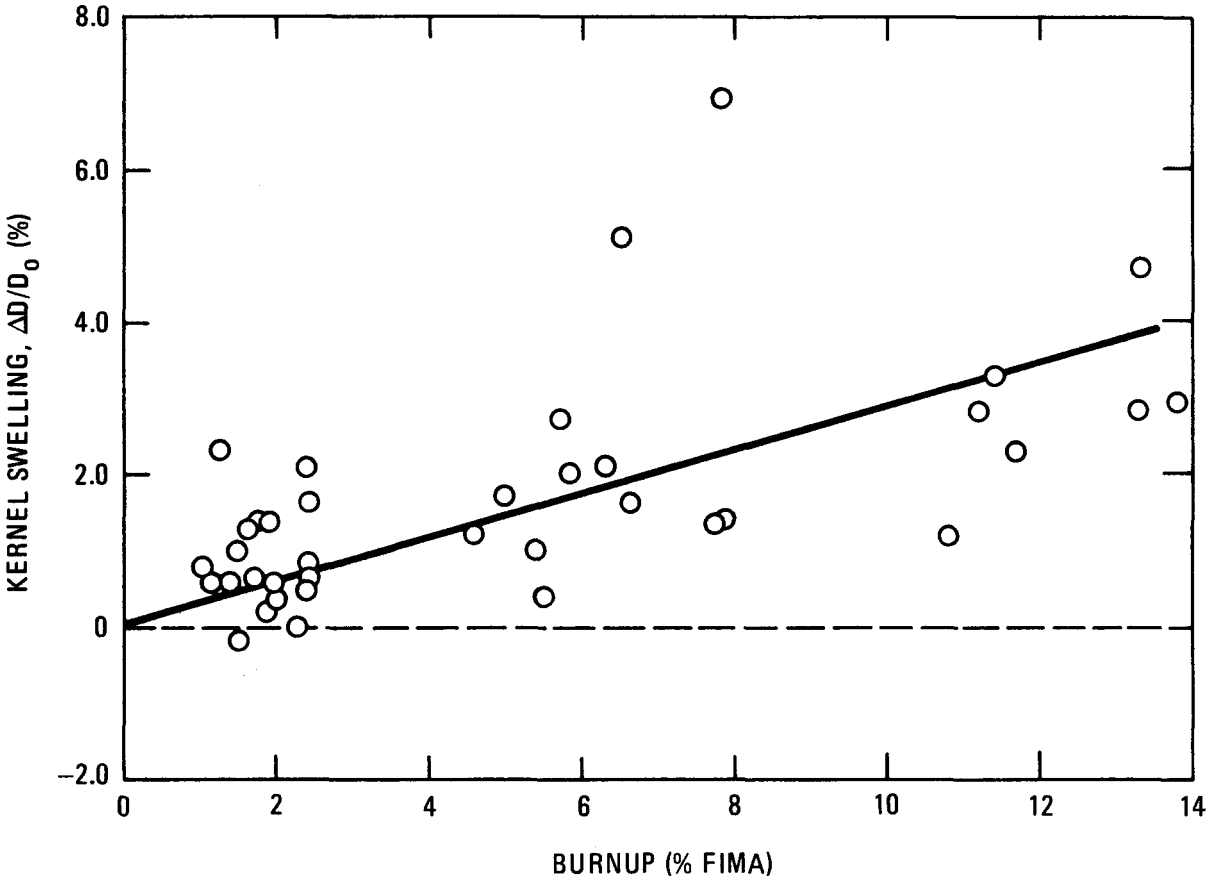


Fig. 14. Fuel kernel swelling as a function of burnup in $ThO_2$ kernels irradiated at 1025° to 1520°C

Table 12. The amount of $ThO_2$ kernel swelling is less than that observed in carbide fuel (Ref. 17). The kernel swelling in both $ThO_2$ and $ThC_2$ fuel is accommodated during irradiation by the low-density buffer coating surrounding the fuel kernels.

## 5.3. IMPLICATIONS FOR LHTGR FUEL SPECIFICATIONS

The HT-12 through HT-15 and HT-17 through HT-19 series of experiments provided the first full burnup irradiation data on LHTGR reference-type BISO $ThO_2$ particles. The irradiation conditions of these experiments were more severe than peak LHTGR design conditions and many of the coated designs tested were nonconservative in order to establish failure criteria required for coated particle performance model studies and to guide future irradiation studies.

These experiments indicated that 500-μm-diameter $ThO_2$ kernels having 60- to 95-μm-thick buffer coatings and 60- to 95-μm-thick OPyC coatings can be fabricated to survive under the most severe irradiation conditions expected in a LHTGR. However, the test results clearly demonstrated that PyC anisotropy, which is a strong function of coating rate, is one of the most important variables affecting the irradiation performance of BISO OPyC coatings. The anisotropy of OPyC coatings deposited at mean coating rates of <2.7 μm/min was high enough to cause failure even during irradiation to moderate fast neutron fluences. Subsequent tests have demonstrated that BISO OPyC coatings must be deposited at batch mean OPyC coating rates ≥4.5 μm/min in coaters similar in design to those used by GA to ensure adequate performance during irradiation to LHTGR peak conditions (Refs. 10, 13).

Once low OPyC coating anisotropies have been obtained, other variables such as density become important in controlling particle performance. In this series of HT experiments a BISO particle batch having an OPyC coating density of 1.94 $Mg/m^3$ exhibited better irradiation performance in the high-temperature magazine than two batches which had OPyC coating densities of

1.82 $Mg/m^3$. These results are consistent with the subsequent data obtained from capsules P13R and P13S, which indicated that BISO OPyC coatings must be restricted to densities $\geq$1.85 $Mg/m^3$ to ensure survival during high-temperature operation and to reduce the permeability of the coating to gaseous fission products (Ref. 13). The permeability of the BISO OPyC coatings prior to irradiation was not assessed. The level of thorium contamination determined by acid leaching for the parent batches ranged from $6.0 \times 10^{-7}$ to $1.1 \times 10^{-4}$ g Th/g Th. However, these values do not represent the degree of OPyC permeability because all batches contained seal coats and the samples tested were carefully selected to avoid defective particles. Postirradiation fission gas release measurements were not performed on intact samples; consequently, a measure of the OPyC coating permeability after irradiation was not obtained either.

In summary, it should be noted that the stress levels in BISO OPyC coatings depend on several variables which include a number of coating properties, burnup, fast neutron fluence, and temperature. A rigorous evaluation of BISO coating performance can only be performed with the aid of particle stress models (Ref. 15). The irradiation data obtained from the HT-12 through HT-15 and HT-17 through HT-19 experiments were used in the initial comparisons of the model with experimental results (Ref. 16).

# 6. SUMMARY AND CONCLUSIONS

The HT capsule irradiation series are evaluation tests of fertile particle coating designs. The data obtained from these accelerated tests provide a good basis for performance model studies. The results of the HT-12 through HT-15 and HT-17 through HT-19 capsule irradiations are summarized as follows:

1. Fertile BISO particles having a 500-μm-diameter $ThO_2$ kernel can be fabricated to survive under the most severe irradiation conditions expected in a LHTGR.

2. Anisotropy of the OPyC coating is one of the most important variables affecting the irradiation performance of BISO coated particles and anisotropy is strongly controlled by OPyC coating rate. At fluences ranging from 6.0 to 10.0 x $10^{25}$ $n/m^2$ and at temperatures <1335°C, particle batches with mean coating rates <2.7 μm/min exhibited high levels of OPyC failure while particle batches with a mean coating rate >3.8 μm/min, with one exception (up to 3% failure), did not experience any OPyC coating failures.

3. High-density OPyC coatings (1.94 $Mg/m^3$) exhibited better irradiation stability at high temperatures than lower density (1.82 $Mg/m^3$) OPyC coatings.

4. One batch of TRISO particles having a 500-μm-diameter $ThO_2$ kernel and nominal coating thicknesses of 95 μm, 28 μm, 29 μm, and 36 μm for the buffer, inner PyC, SiC, and OPyC coatings, respectively, was tested to provide guidance for further design improvements. The high levels of pressure vessel failure observed after irradiation to moderate exposures indicate that this particle design is nonconservative.

5. Irradiation-induced diametral $ThO_2$ kernel swelling increased with increasing burnup and ranged from -0.2% to +6.9% for burnups between 1.0 and 13.8% FIMA and temperatures of 1025° to 1520°C.

6. Irradiation-induced BISO particle dimensional changes were correlated with burnup and fast neutron fluence. Total particle volume changes on the order of -12% to -17% were observed at the full HTGR fluence of $8.0 \times 10^{25}$ $n/m^2$ $(E > 29\ fJ)_{HTGR}$.

ACKNOWLEDGMENTS

The author would like to acknowledge the contributions of the many people at GA and ORNL who assisted with the fabrication, irradiation, and postirradiation examination of capsules HT-12 through HT-15 and HT-17 through HT-19. In particular, I would like to acknowledge the Fuel Process and Manufacturing Division personnel at GA for fuel sample preparation; C. L. Smith and D. P. Harmon for development of the experimental test matrix, sample selection, and many helpful discussions; E. V. Hoshi and W. E. Simpson for hot cell analytical studies; E. E. Anderson for the heavy metal burnup calculations; and M. J. Kania of ORNL for the thermal analysis. The helpful discussions and data analysis provided by E. L. Long, Jr., and B. H. Montgomery of ORNL and editing of the manuscript by Jean Jayne are also greatly appreciated.

## REFERENCES


1. "Gas-Cooled Reactor Programs Annual Progress Report for the Period Ending December 31, 1973," ERDA Report ORNL-4975, Oak Ridge National Laboratory, April 1976, pp. 127-138.
2. "HTGR Fuels and Core Development Program Quarterly Progress Report for the Period Ending August 30, 1974," ERDA Report GA-A13126, General Atomic Company, September 30, 1974.
3. Kerr, H. T., E. J. Allen, and D. L. Reed, "Lattice Displacement Calculations and Comparisons for Different Irradiation Facilities," ERDA Report ORNL-TM-5269, Oak Ridge National Laboratory, March 1976.
4. Scott, C. B., and D. P. Harmon, "Postirradiation Examination of Capsules HRB-4, HRB-5, and HRB-6," ERDA Report GA-A13267, Appendix A, General Atomic Company, November 28, 1975.
5. Kania, M. J., "HTCAP - A Fortran IV Program for Calculating Coated Particle Operating Temperatures in HFIR Target Irradiation Experiments," ERDA Report ORNL-TM-5332, Oak Ridge National Laboratory, May 1976.
6. Canada, D. C., and W. R. Laing, "Use of a Density Gradient Column to Measure the Density of Microspheres," Anal. Chem. 39, 691 (1967).
7. Stevens, D. W., "Optical Anisotropy and Preferred Orientation in Nearly Isotropic Pyrocarbons," General Atomic Report GA-A13307, January 22, 1975.
8. Bokros, J. C., and R. J. Price, "Radiation-Induced Dimensional Changes in Pyrolytic Carbons Deposited in a Fluidized Bed," Carbon 4, 441 (1966).
9. Harmon, D. P., and C. B. Scott, "Development and Irradiation Performance of LHTGR Fuel," ERDA Report GA-A13173, General Atomic Company, October 31, 1975.
10. Harmon, D. P., and C. B. Scott, "Properties Influencing HTGR Coated Fuel Particle Performance," ERDA Report GA-A14105, General Atomic Company, March 1977; also to be published in Nuclear Technology.

11. Koss, P., and K. Wallish, "Optical Determination of the Anisotropy of Pyrocarbon," in Proceedings of International Carbon Conference, Baden-Baden, Germany, June 25-30, 1972, pp. 256-258.
12. "HTGR Base Program Quarterly Progress Report for the Period Ending August 31, 1973," USAEC Report Gulf-GA-A1275, Gulf General Atomic, September 28, 1973.
13. Scott, C. B., D. P. Harmon, and J. F. Holzgraf, "Postirradiation Examination of Capsules P13R and P13S," ERDA Report GA-A13827, General Atomic Company, October 8, 1976.
14. Scott, C. B., and D. P. Harmon, "Postirradiation Examination of Capsule F-30," General Atomic Report GA-A13208, April 1, 1975.
15. Kaae, J. L., "The Mechanical Behavior of BISO Coated Fuel Particles During Irradiation, Part I," ERDA Report GA-A14052, General Atomic Company, July 1976.
16. Kaae, J. L., R. E. Bullock, C. B. Scott, and D. P. Harmon, "The Mechanical Behavior of BISO Coated Fuel Particles During Irradiation, Part II," ERDA Report GA-A14052, General Atomic Company, July 1976.
17. Stansfield, O. M., T. D. Gulden, and D. P. Harmon, "Fuel Kernel Materials for the Thorium Cycle HTGR," in Proceedings of the International Conference on Nuclear Fuel Performance, British Nuclear Energy Society, London, October 15-19, 1973, Paper 35 (CONF 731004).

# APPENDIX

## REPRESENTATIVE PREIRRADIATION PHOTOMICROGRAPHS OF THE COATED PARTICLE BATCHES TESTED IN THE HT-12 THROUGH HT-15 AND HT-17 THROUGH HT-19 CAPSULE SERIES

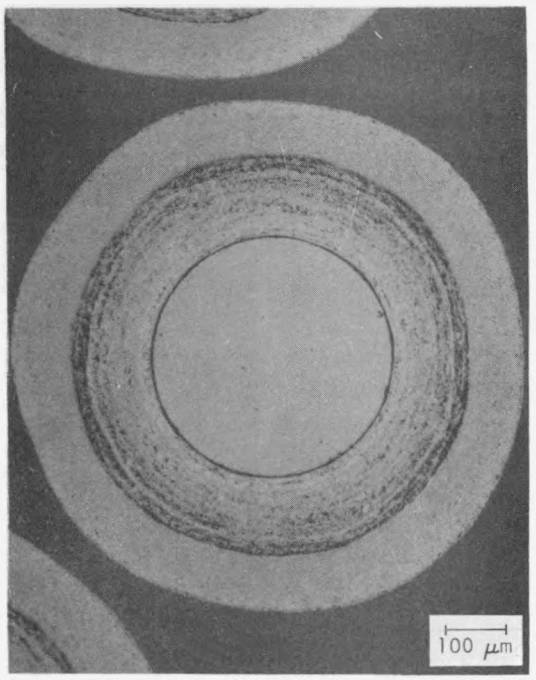


M38811-5 (a)

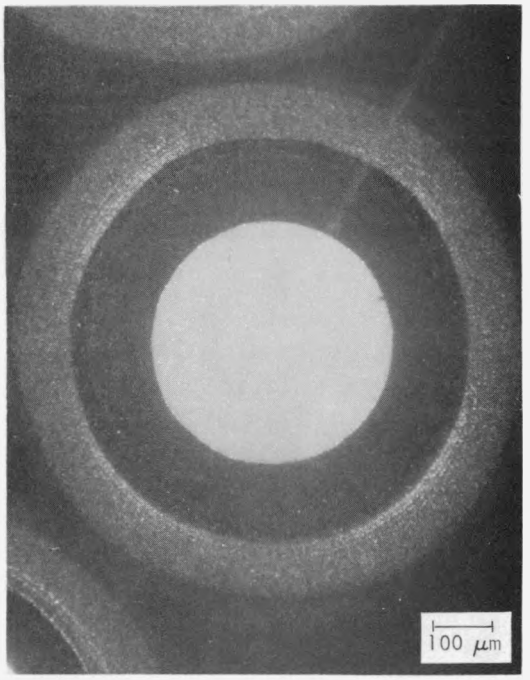


M38811-6 (b)

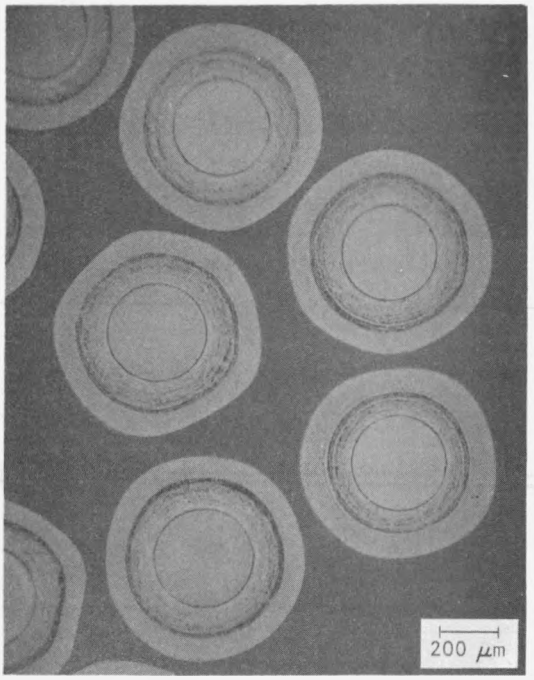


M38811-3 (c)

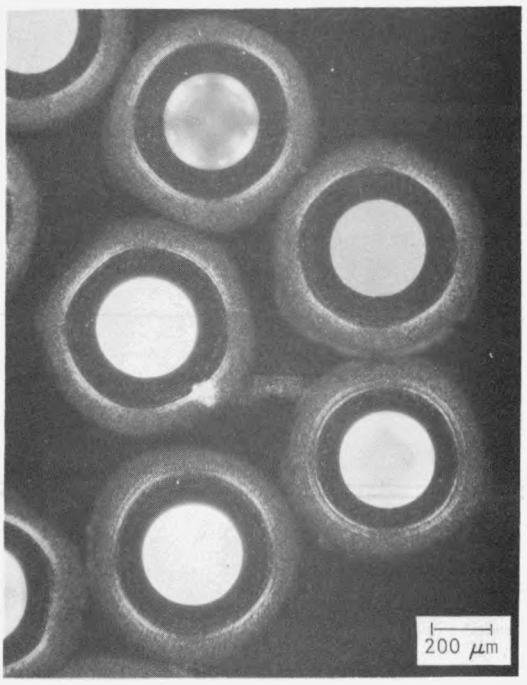


M38811-4 (d)

Fig. A-1. Preirradiation photomicrographs of BISO coated $ThO_2$ particles from batch 4252-00-013: (a) and (c) bright field; (b) and (d) polarized light. High-density regions in the OPyC coating appear bright under polarized light.

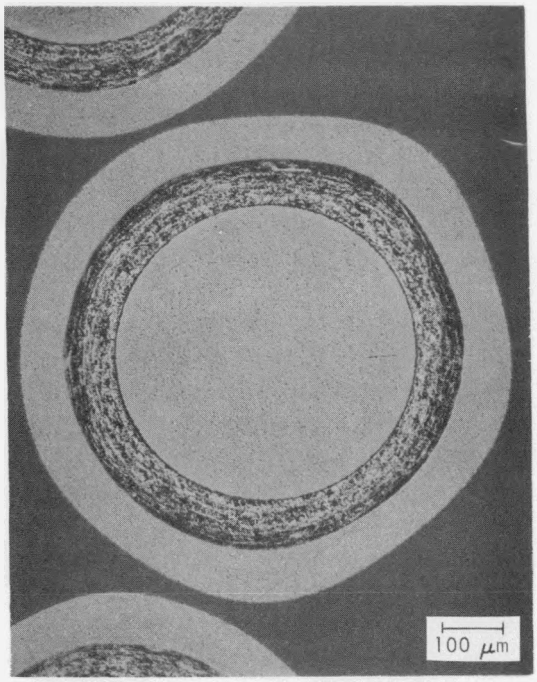


M38810-4 (a)

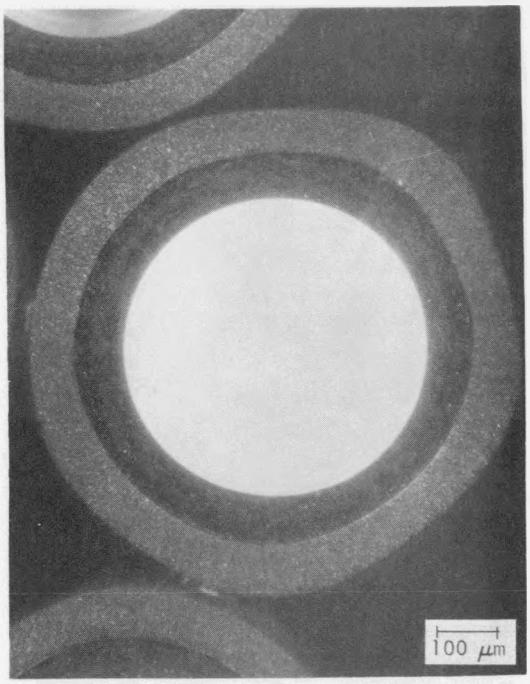


M38810-5 (b)

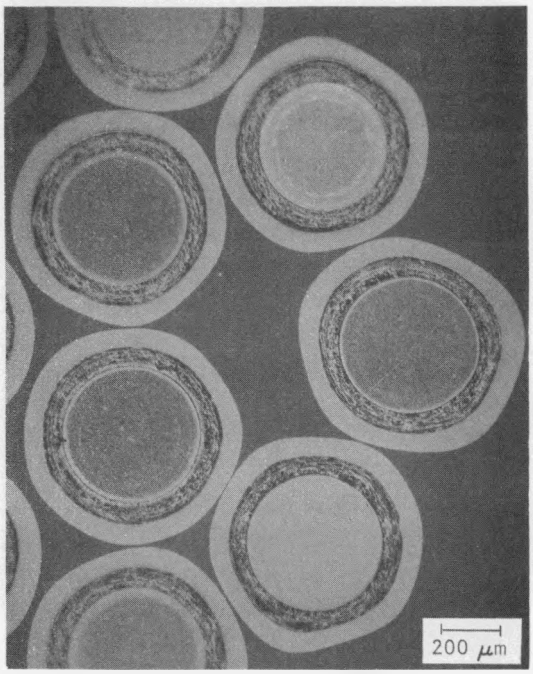


M38810-1 (c)

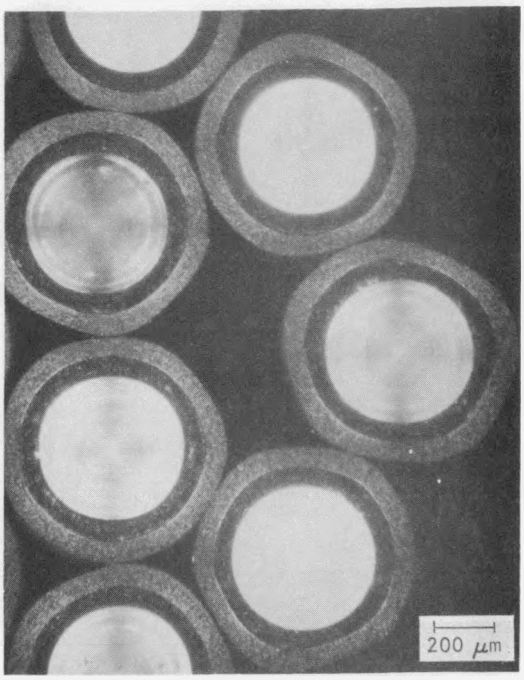


M38810-2 (d)

Fig. A-2. Preirradiation photomicrographs of BISO coated $ThO_2$ particles from batch 4252-01-071: (a) and (c) bright field; (b) and (d) polarized light

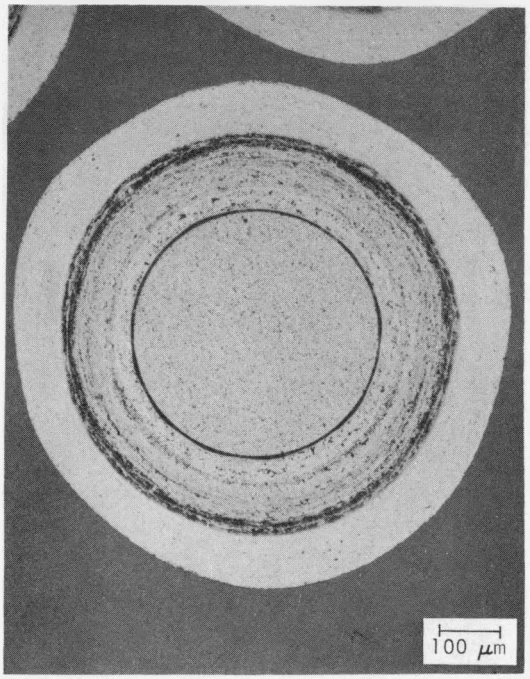


M38812-5 (a)

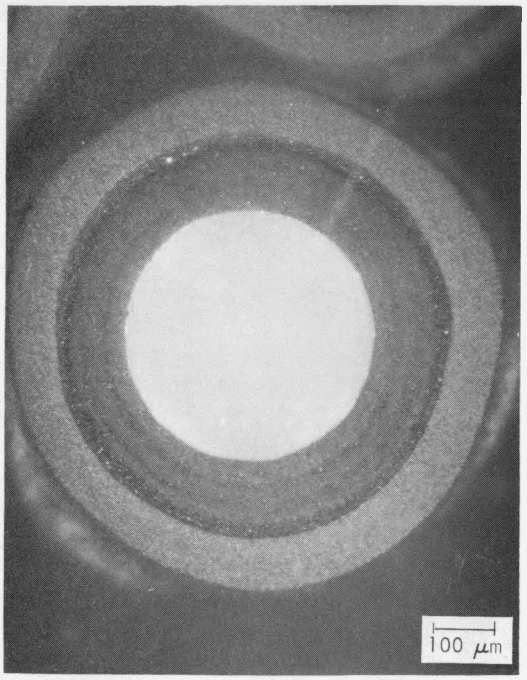


M38812-6 (b)

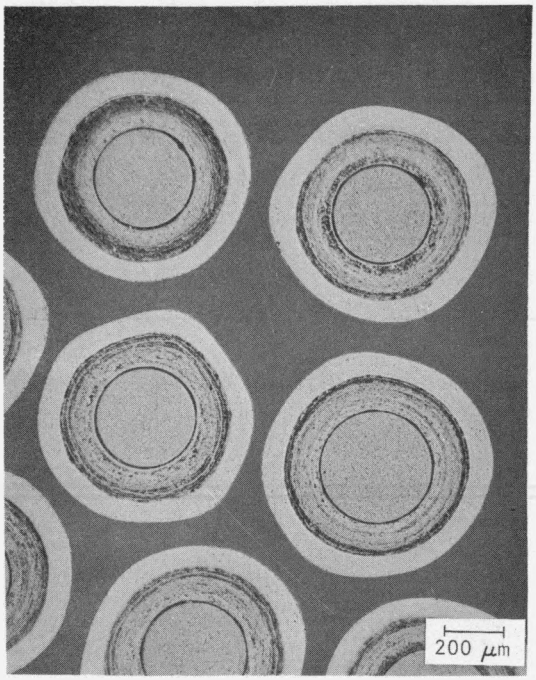


M38812-1 (c)

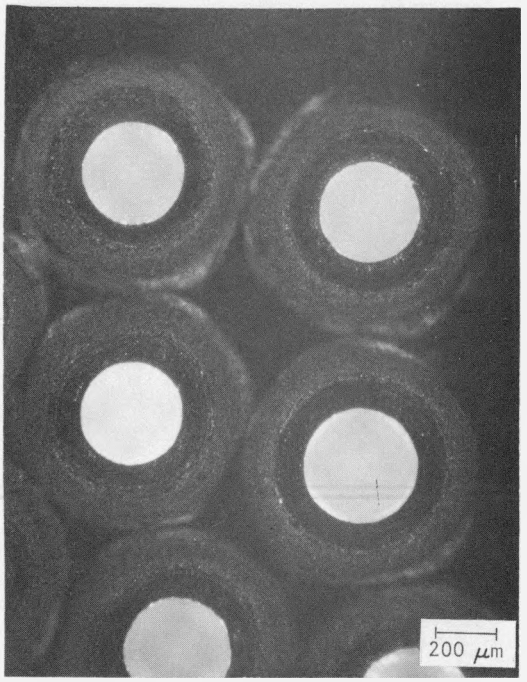


M38812-2 (d)

Fig. A-3. Preirradiation photomicrographs of BISO coated $ThO_2$ particles from batch 4252-01-015: (a) and (c) bright field; (b) and (d) polarized light

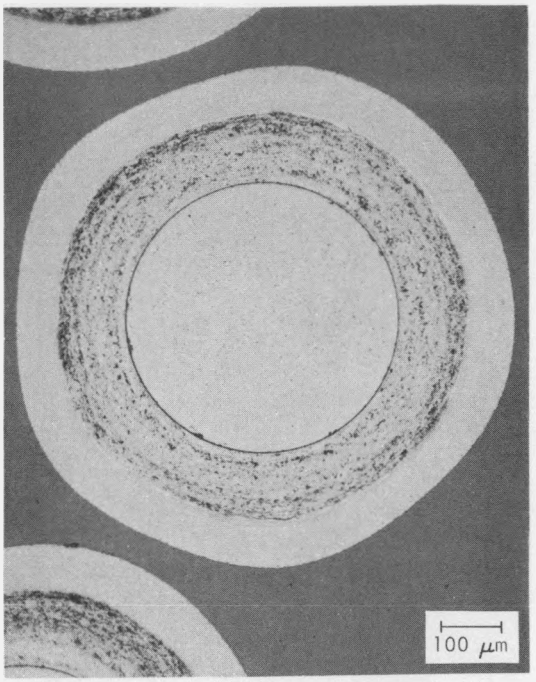


M38813-5 (a)

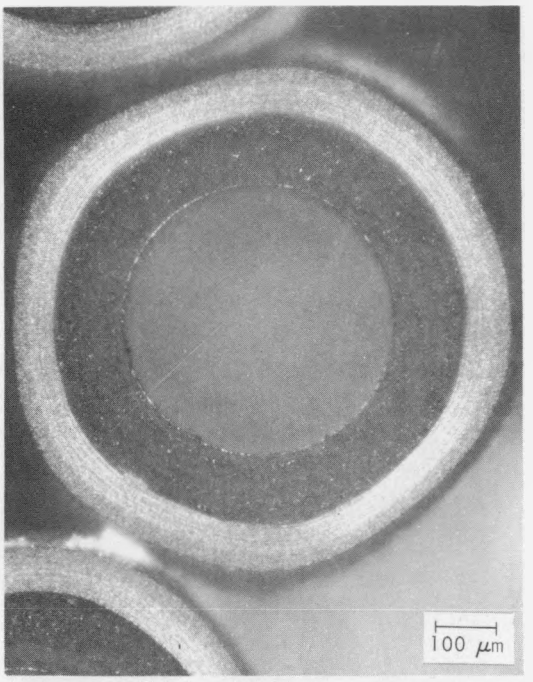


M38813-6 (b)

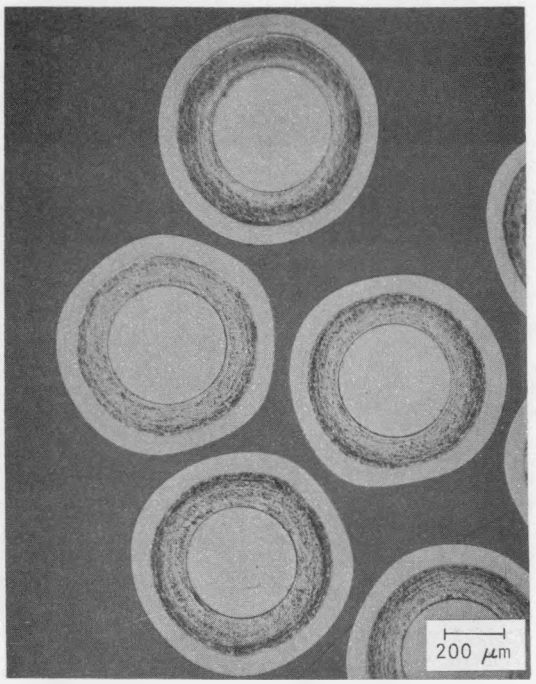


M38813-1 (c)

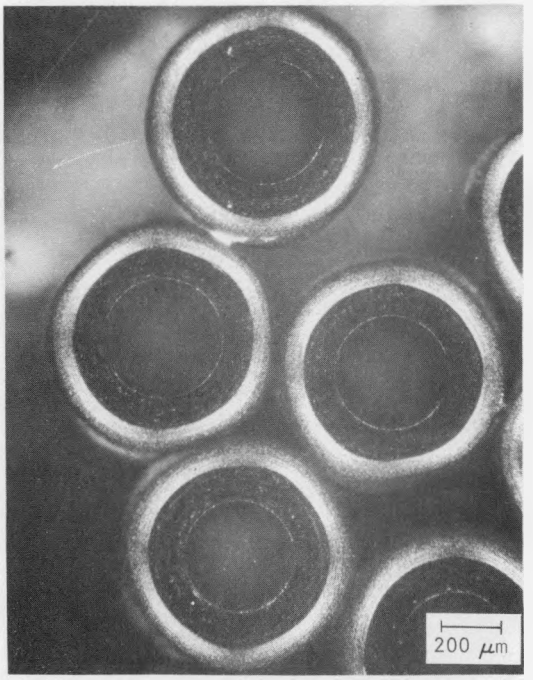


M38813-2 (d)

Fig. A-4. Preirradiation photomicrographs of BISO coated $ThO_2$ particles from batch 4252-03-012: (a) and (c) bright field; (b) and (d) polarized light. High-density regions in the OPyC coating appear bright under polarized light.

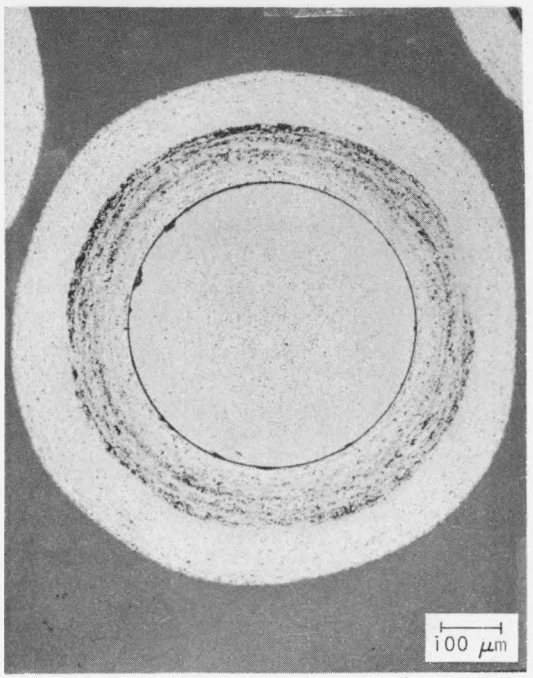


M38814-5 (a)

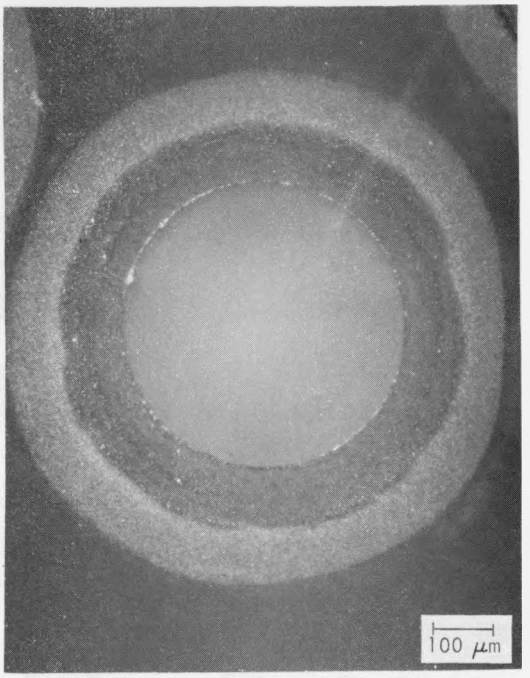


M38814-6 (b)

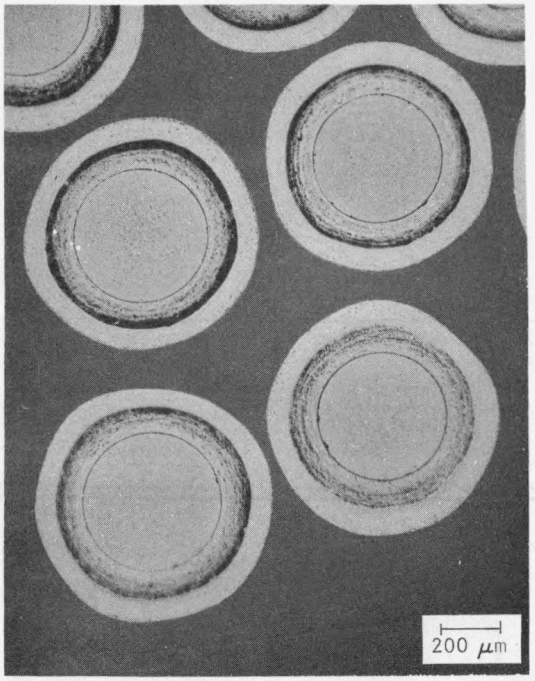


M38814-1 (c)

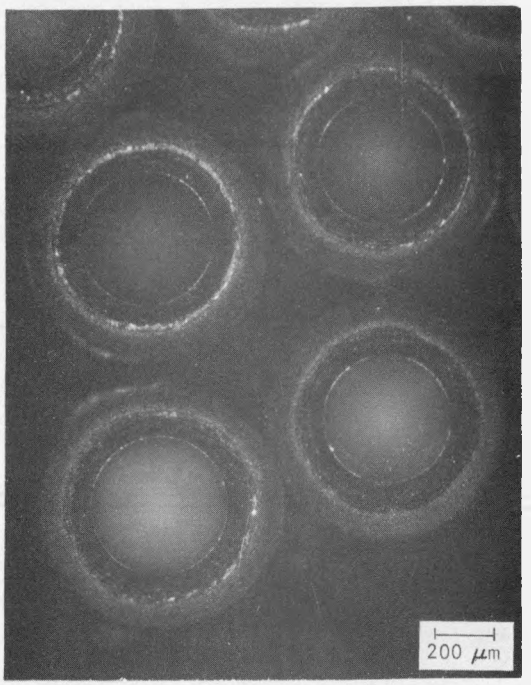


M38814-2 (d)

Fig. A-5. Preirradiation photomicrographs of BISO coated $ThO_2$ particles from batch 4252-06-012: (a) and (c) bright field; (b) and (d) polarized light

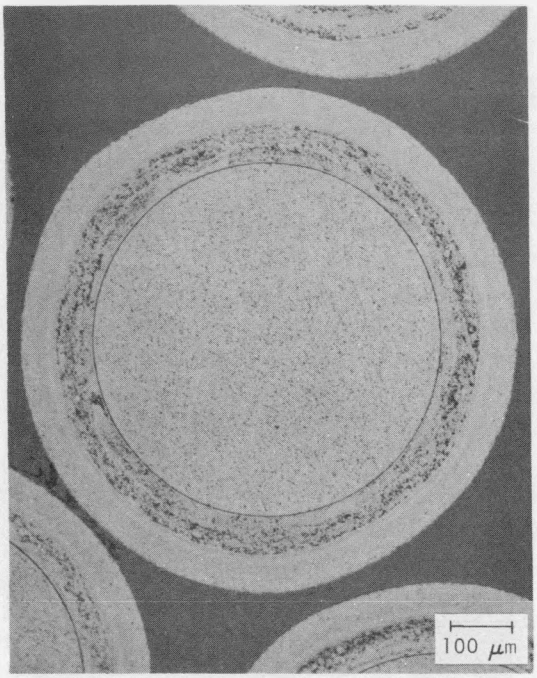


M38815-7 (a)

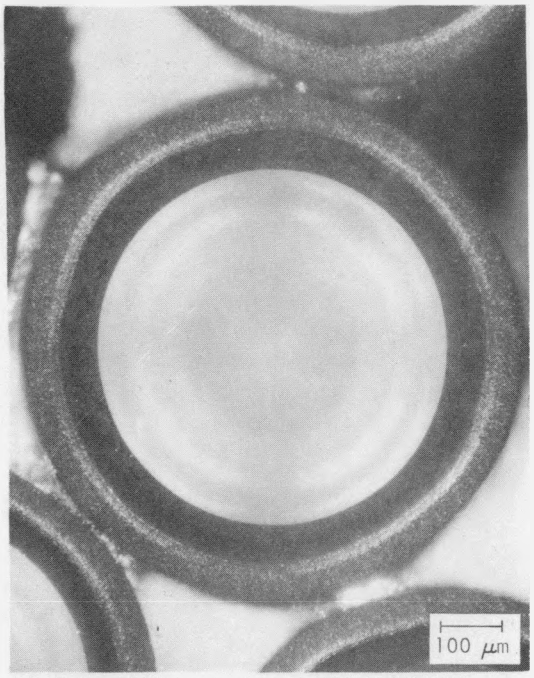


M38815-8 (b)

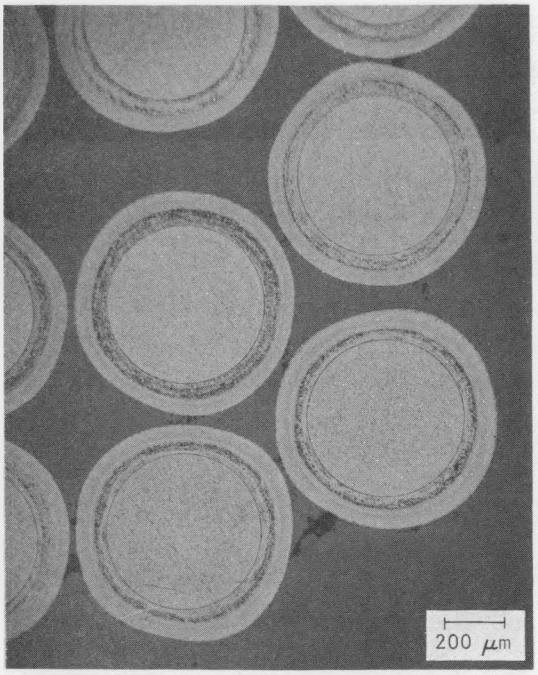


M38815-1 (c)

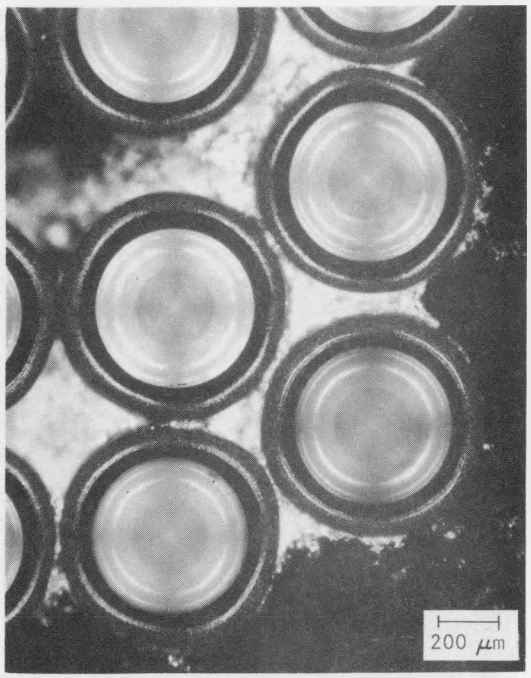


M38815-2 (d)

Fig. A-6. Preirradiation photomicrographs of BISO coated $ThO_2$ particles from batch 4252-07-016: (a) and (c) bright field; (b) and (d) polarized light. High-density regions in the OPyC coating appear bright under polarized light.

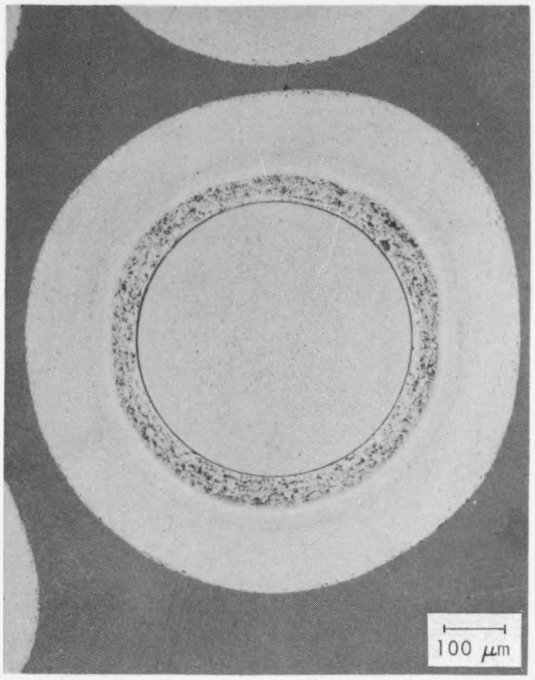


M38816-7 (a)

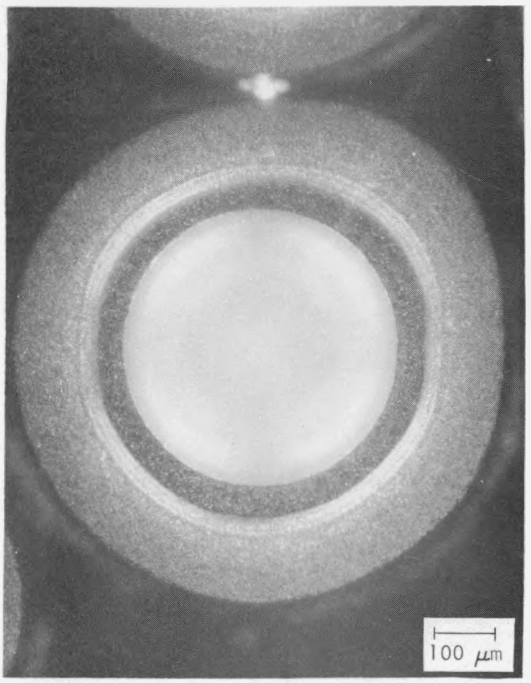


M38816-8 (b)

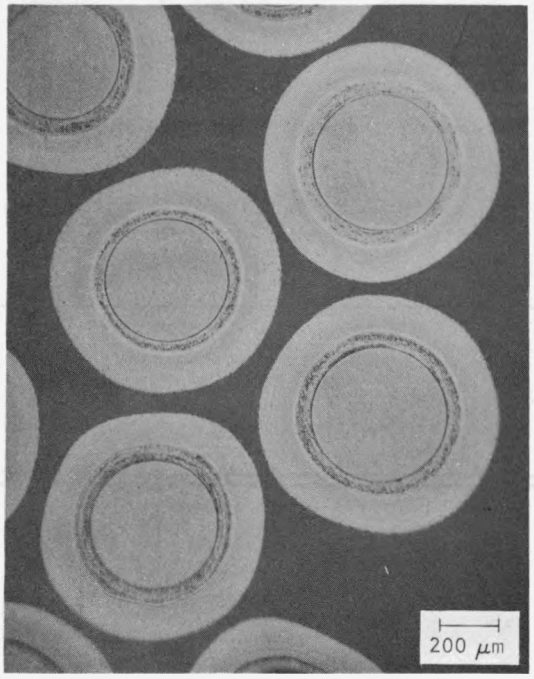


M38816-3 (c)

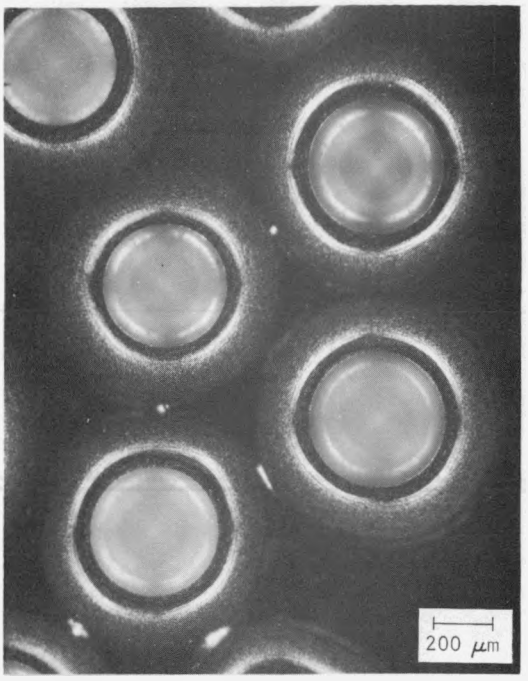


M38816-4 (d)

Fig. A-7. Preirradiation photomicrographs of BISO coated $ThO_2$ particles from batch 4252-08-014: (a) and (c) bright field; (b) and (d) polarized light. High-density regions in the OPyC coating appear bright under polarized light.

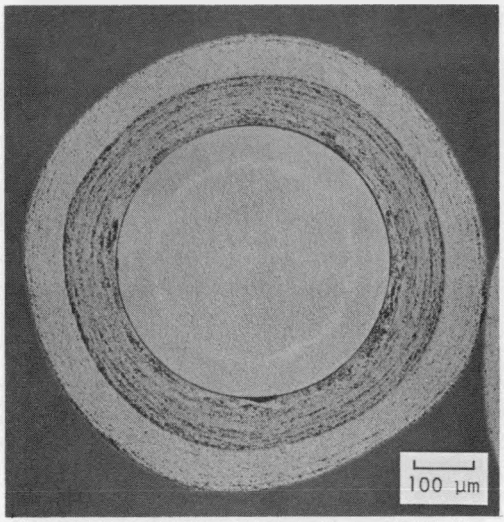


M39929-7 (a)

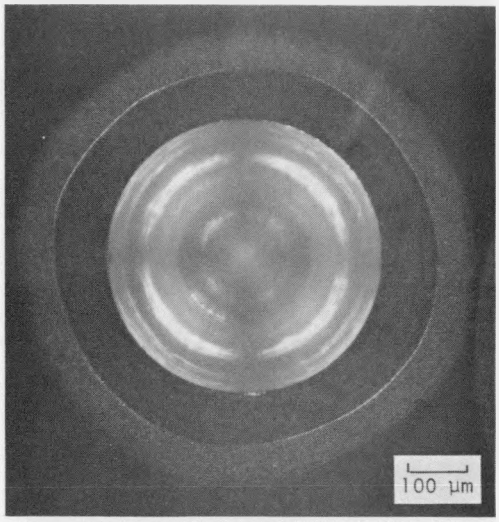


M39929-8 (b)

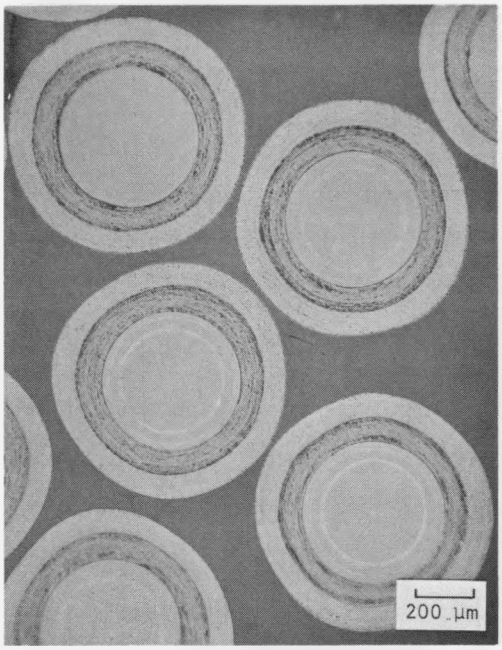


M39929-1 (c)

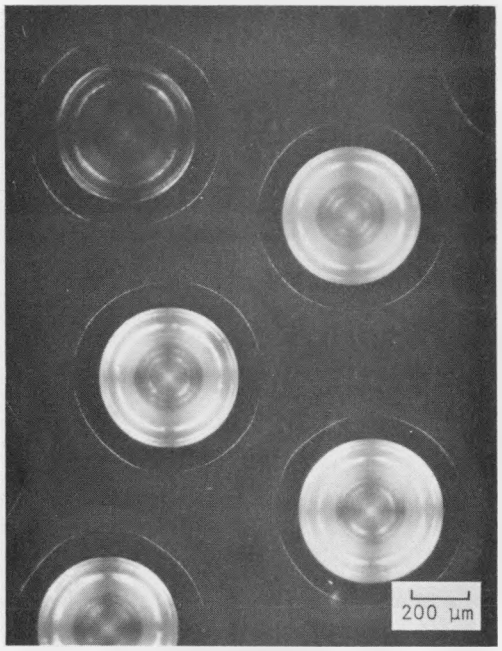


M39929-2 (d)

Fig. A-8. Preirradiation photomicrographs of BISO coated $ThO_2$ particles from batch 6542-01-013: (a and c) bright field and (b and d) polarized light

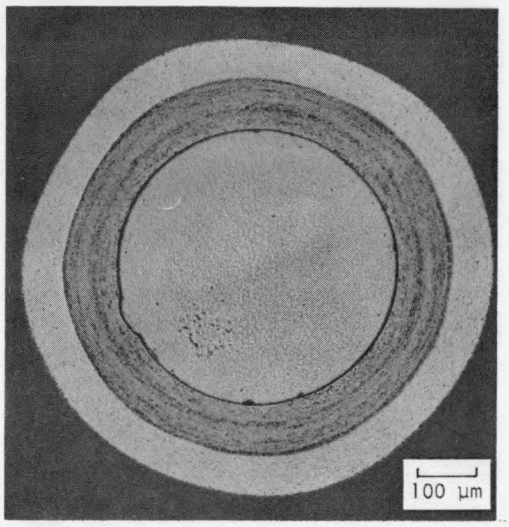


M39935-7 (a)

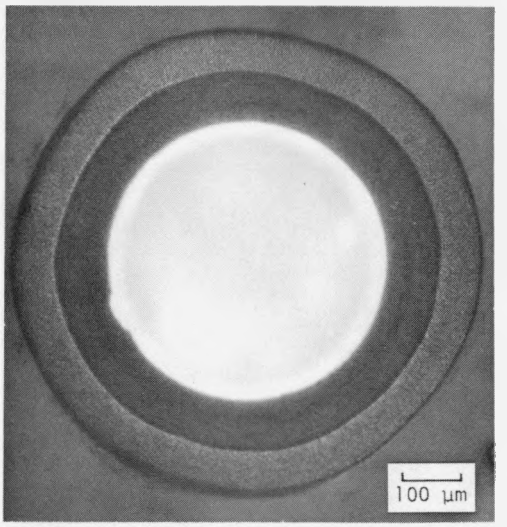


M39935-8 (b)

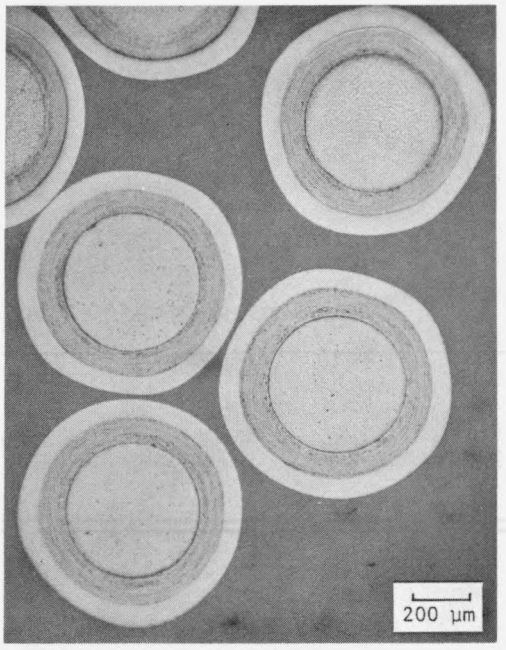


M39935-1 (c)

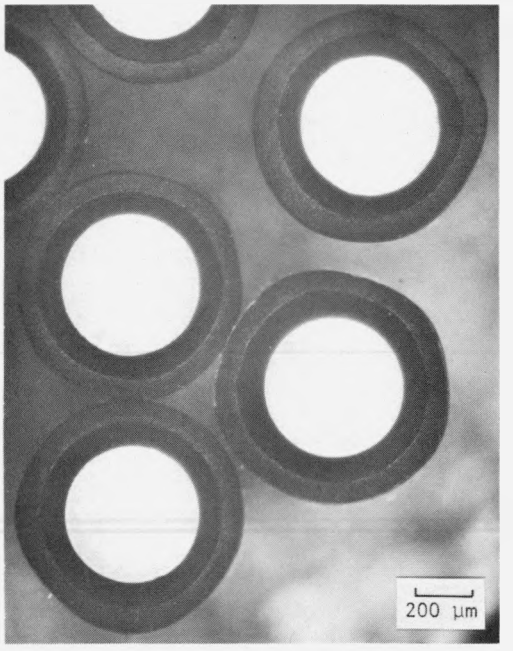


M39935-2 (d)

Fig. A-9. Preirradiation photomicrographs of BISO coated $ThO_2$ particles from batch 6542-01-023: (a and c) bright field and (b and d) polarized light

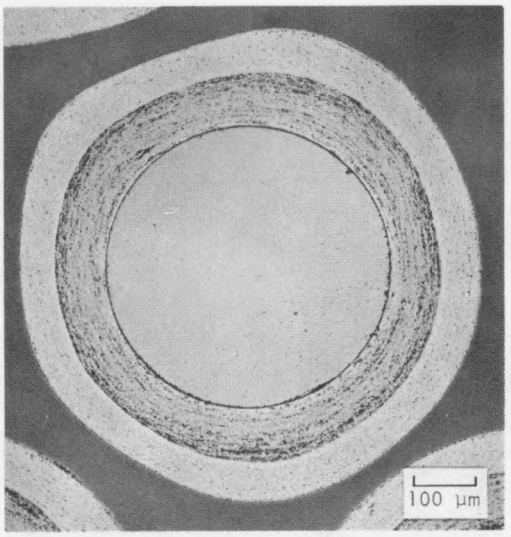


M39931-1 (a)

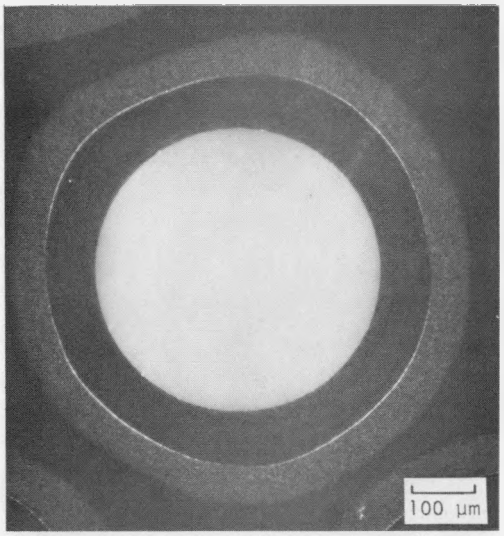


M39931-2 (b)

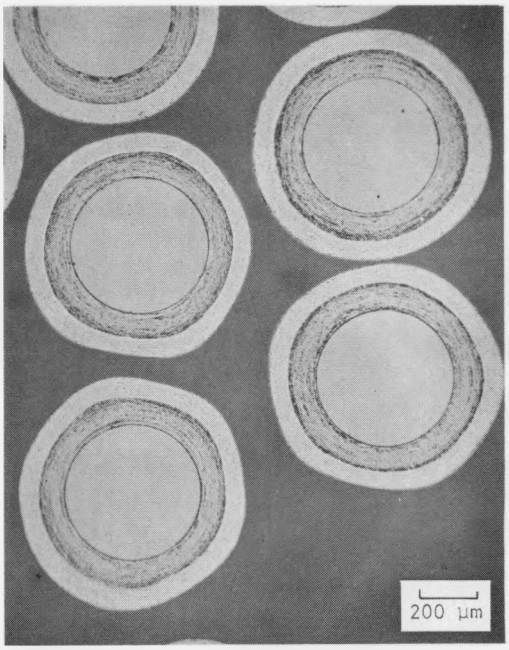


M39931-6 (c)

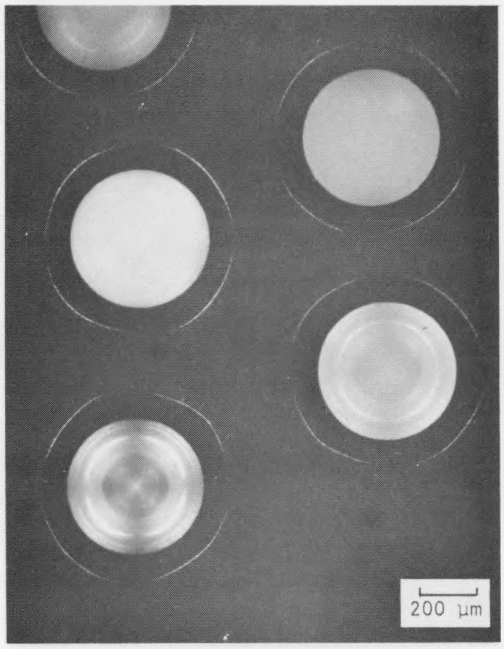


M39931-7 (d)

Fig. A-10. Preirradiation photomicrographs of BISO coated $ThO_2$ particles from batch 6542-02-023: (a and b) bright field and (b and d) polarized light

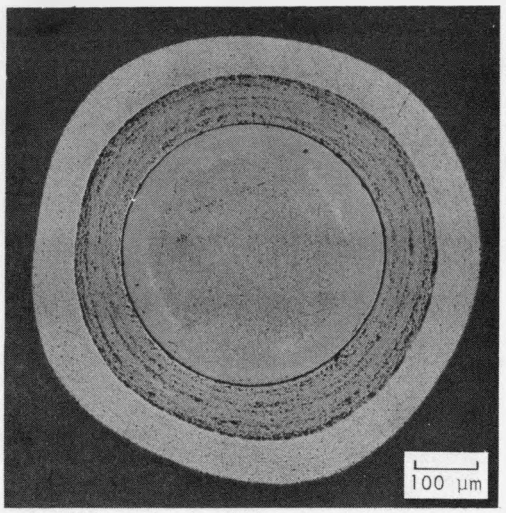


M39932-10 (a)

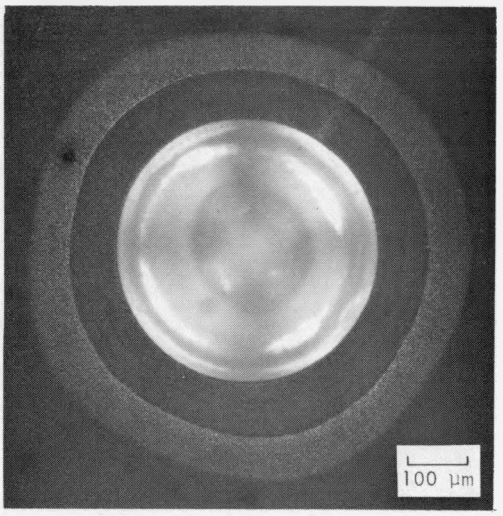


M39932-11 (b)

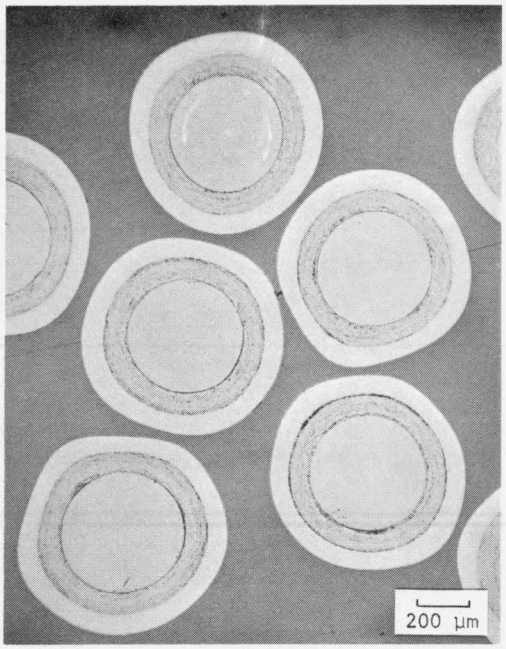


M39932-1 (c)

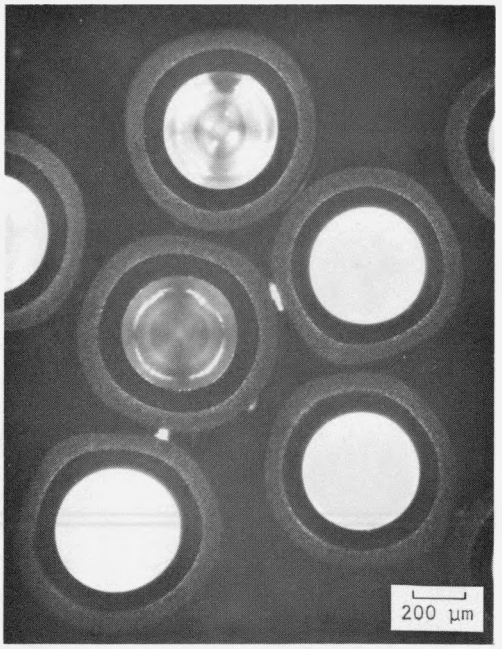


M39932-2 (d)

Fig. A-11. Preirradiation photomicrographs of BISO coated $ThO_2$ particles from batch 6542-02-033: (a and c) bright field and (b and d) polarized light

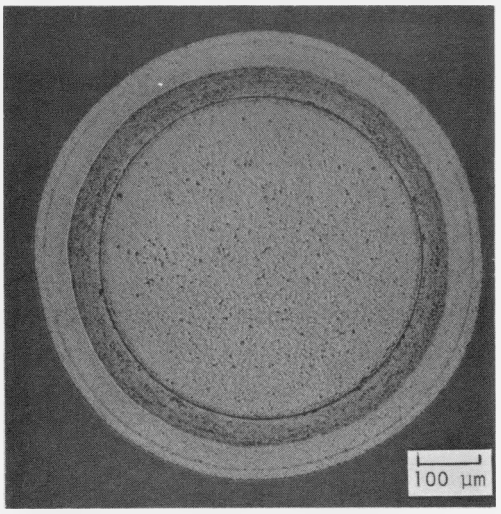


M39933-11 (a)

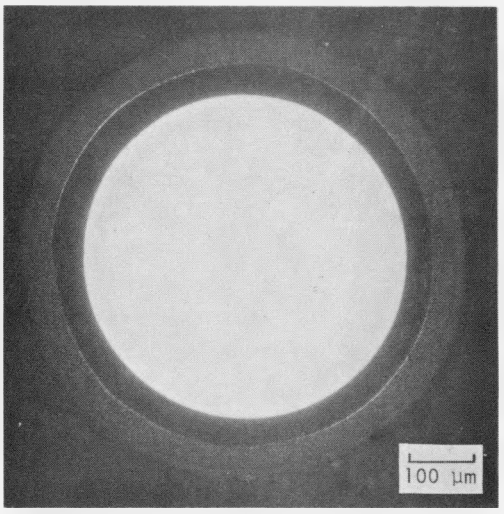


M39933-12 (b)

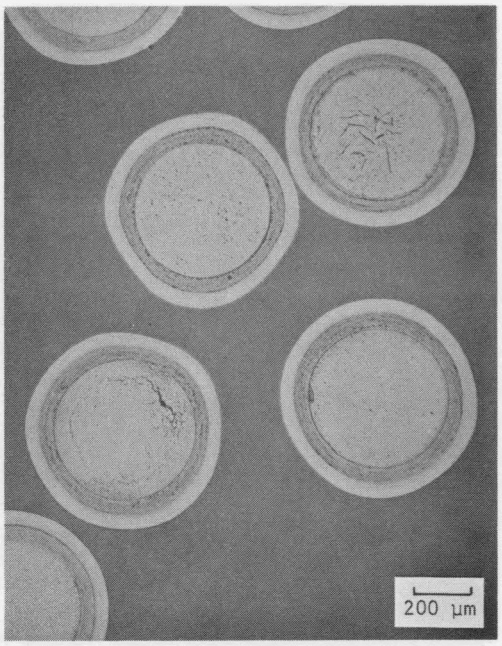


M39933-3 (c)

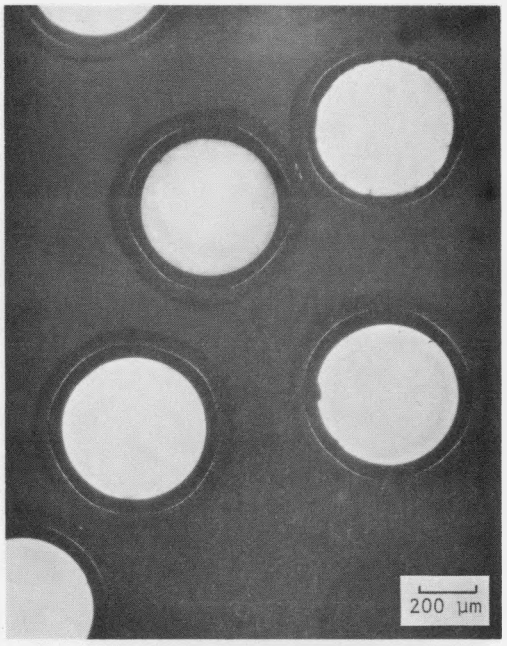


M39933-4 (d)

Fig. A-12. Preirradiation photomicrographs of BISO coated $ThO_2$ particles from batch 6542-16-013: (a and c) bright field and (b and d) polarized light

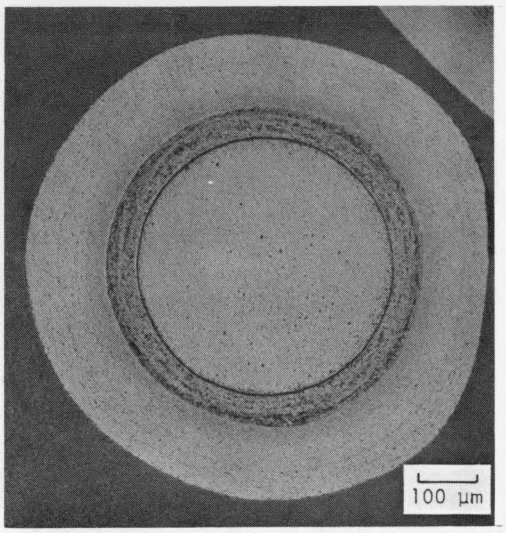


M39934-10 (a)

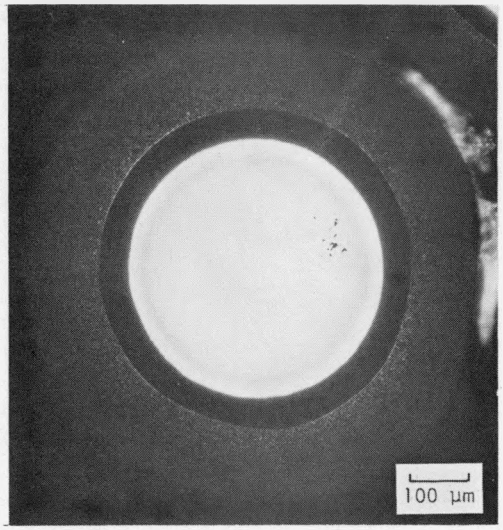


M39934-11 (b)

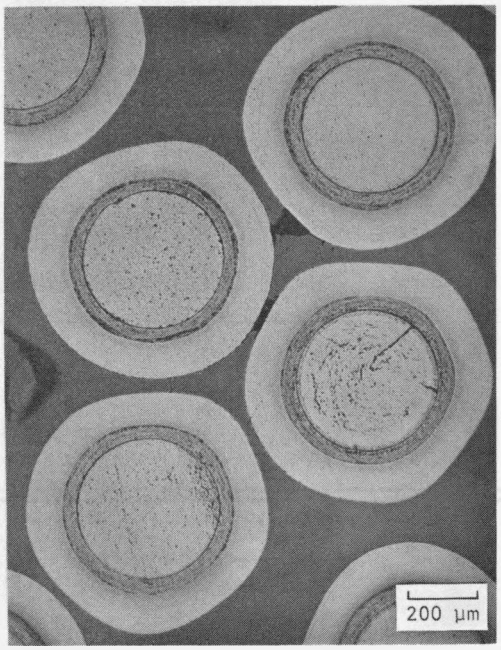


M39934-4 (c)

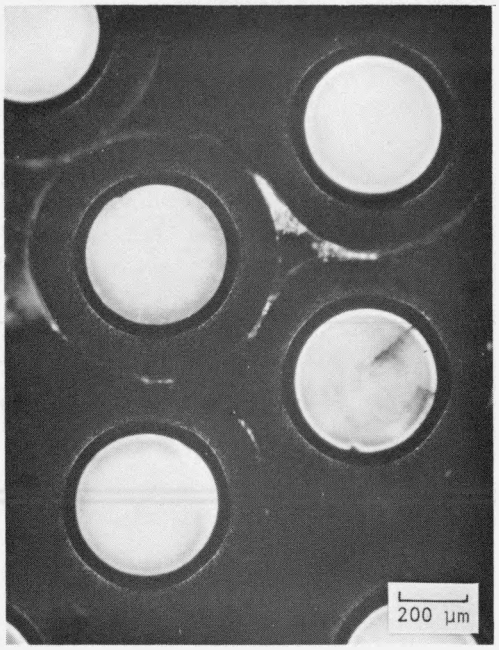


M39934-5 (d)

Fig. A-13. Preirradiation photomicrographs of BISO coated $ThO_2$ particles from batch 6542-17-013: (a and c) bright field and (b and d) polarized light

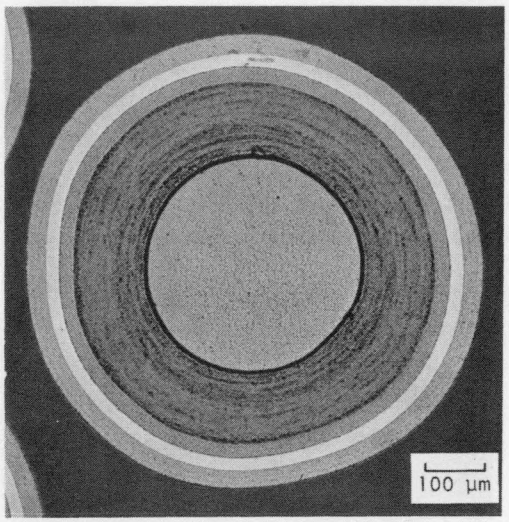


M39930-7 (a)

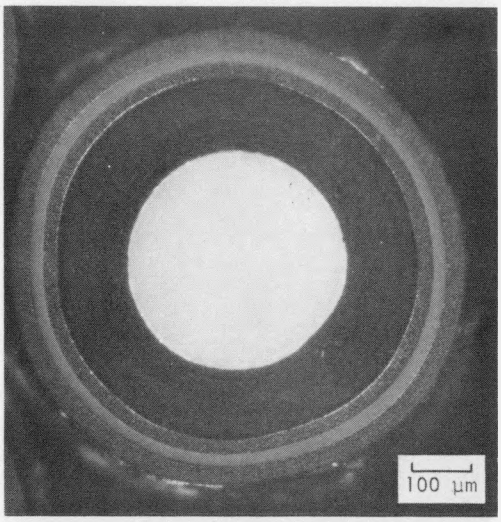


M39930-8 (b)

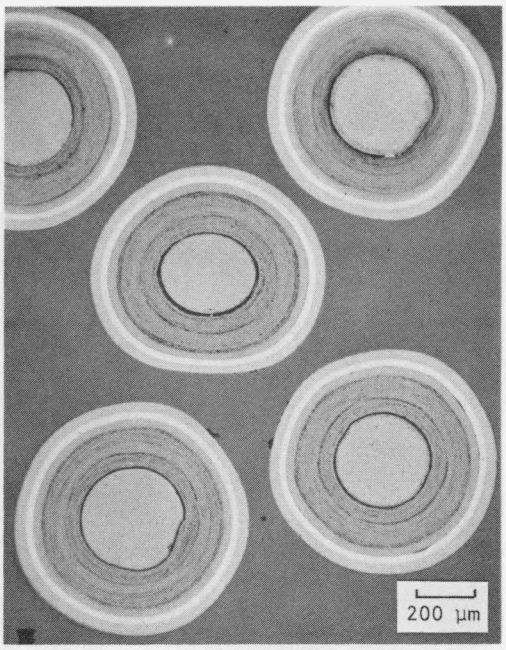


M39930-1 (c)

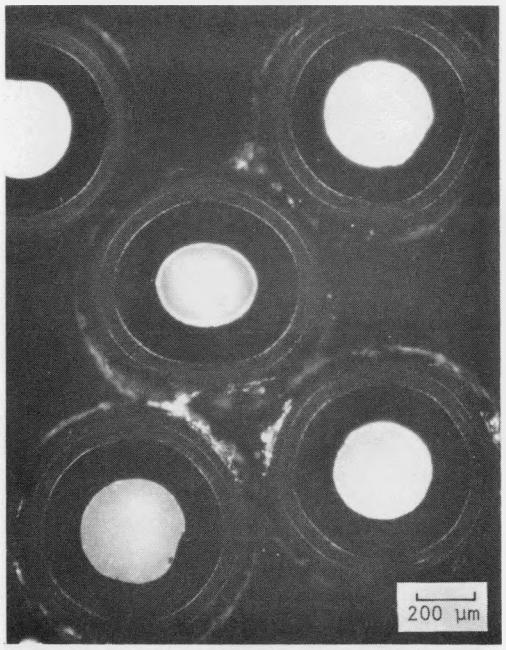


M39930-2 (d)

Fig. A-14. Preirradiation photomicrographs of TRISO coated $ThO_2$ particles from batch 6252-01-023: (a and c) bright field and (b and d) polarized light